

A Gas Cherenkov Muon Spectrometer for Nuclear Security Applications

Junghyun Bae, Ph.D.

School of Nuclear Engineering, Purdue University

Eugene P. Wigner Distinguished Staff Fellow, Oak Ridge National Laboratory

USA

27 July 2022



Some Housekeeping Items



Listen through your computer

Please select the “mic and speakers” radio button on the right-hand audio and pane display



Technical Difficulties

Search the Go To Webinars Support:
<https://support.goto.com/webinar>



To ask a question

Select the “Questions” pane on your screen and type in your question



Share with others or watch it again

A video/audio recording of the webinar and the slide decks will be made available at www.gen-4.org



Please take the survey

A brief online survey will follow the webinar.

To Ask a Question

Click Here



To Open the
Go To
Webinar
Control Panel

A screenshot of a GoToWebinar interface. The top part shows a menu with icons for back, microphone, chat, and hand up. Below this is a banner with flags of Brazil, South Africa, and others. The main content area is divided into two panes. The top pane is titled 'Audio' and shows settings for 'Computer audio', 'Phone call', and 'No audio'. It also indicates 'MUTED' and shows the microphone and speaker levels. The bottom pane is titled 'Questions' and contains a text input field with the placeholder text '[Enter a question for staff]' and a 'Send' button. A red circle highlights the 'Questions' pane, and a red arrow points from the text 'Write question in bottom box and hit "Send"' to the 'Send' button.

Write question in bottom box
and hit "Send"

A Gas Cherenkov Muon Spectrometer for Nuclear Security Applications

Junghyun Bae, Ph.D.

School of Nuclear Engineering, Purdue University

Eugene P. Wigner Distinguished Staff Fellow, Oak Ridge National Laboratory

USA

27 July 2022

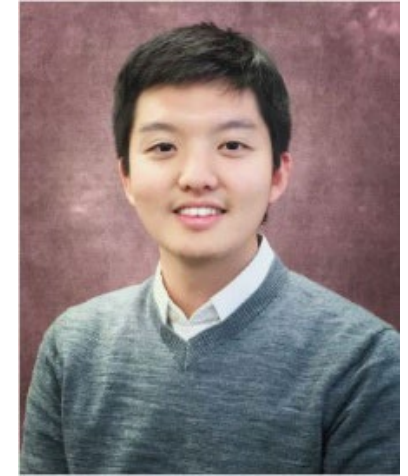


Meet the Presenter

Dr. Junghyun Bae recently completed his Ph.D. at the School of Nuclear Engineering at Purdue University. He will join the Used Fuel and Nuclear Material Disposition group of the Nuclear Energy and Fuel Cycle Division at the Oak Ridge National Laboratory as a *Eugene P. Wigner Distinguished Staff Fellow*.

His research focuses on the development of a high-resolution fieldable muon spectrometer using multi-layer pressurized gas Cherenkov radiators and its applications, i.e., muon tomography, nuclear security, Spent Nuclear Fuel (SNF) casks imaging. He earned his M.S degree in nuclear engineering from the University of California, Berkeley and his B.S. degree in Nuclear and Quantum Engineering from the Korea Advanced Institute of Science and Technology (KAIST).

Dr. Bae won the 'Pitch Your PhD' competition during the 2021 ANS Winter Meeting and Technology Expo in Washington, D.C. He has also been nominated and awarded the Roy G. Post Foundation scholarship, ANS, and KSEA graduate scholarships for his contribution to the safe management of nuclear materials.



A Gas Cherenkov Muon Spectrometer for Nuclear Security Applications

TABLE OF CONTENTS

- I. INTRODUCTION**
 - 1. Motivation
 - 2. Problem Statement
 - 3. Research Objective
- II. MUON SPECTROMETER USING GAS CHERENKOV RADIATORS**
 - 1. Operational Principle
 - 2. Optical Photon Emission
 - 3. Results
- III. MOMENTUM INTEGRATED IMAGING ALGORITHM**
- IV. MOMENTUM INTEGRATED MUON TOMOGRAPHY**
 - 1. Implementation of Cherenkov muon spectrometer in SNF monitoring
 - 2. Results
- V. SUMMARY AND CONCLUSION**

A Gas Cherenkov Muon Spectrometer for Nuclear Security Applications

TABLE OF CONTENTS

- I. INTRODUCTION**
 - 1. Motivation
 - 2. Problem Statement
 - 3. Research Objective
- II. MUON SPECTROMETER USING GAS CHERENKOV RADIATORS**
 - 1. Operational Principle
 - 2. Optical Photon Emission
 - 3. Results
- III. MOMENTUM INTEGRATED IMAGING ALGORITHM**
- IV. MOMENTUM INTEGRATED MUON TOMOGRAPHY**
 - 1. Implementation of Cherenkov muon spectrometer in SNF monitoring
 - 2. Results
- V. SUMMARY AND CONCLUSION**

I. Introduction

1. Motivation

- Muon tomography has been emerged as one of promising non-invasive monitoring and imaging techniques for dense and large objects.
- Cosmic ray muons have benefits over traditional induced radiation probes for non-destructive imaging due to their high-energy (10⁹~12 eV vs 10³~6 eV)
- For example,
 - Spent nuclear fuel cask imaging
 - Nuclear reactor (e.g., monitoring damaged reactor core in Fukushima nuclear site)
 - Nuclear materials inspection in a cargo container
 - Archeology (e.g., finding a hidden chamber in the Great Pyramid of Giza)
 - Geotomography (e.g., investigating magma chamber underneath volcano to predict upcoming eruption)

I. INTRODUCTION

2. Problem Statement

- Benefits of measuring muon momentum in muon applications (monitoring and imaging) has been explored.
- Therefore, often a mean cosmic ray muon momentum value (3–4 GeV/c) represents the entire spectrum.
- Because none of existing muon spectrometers can be deployed in the field.

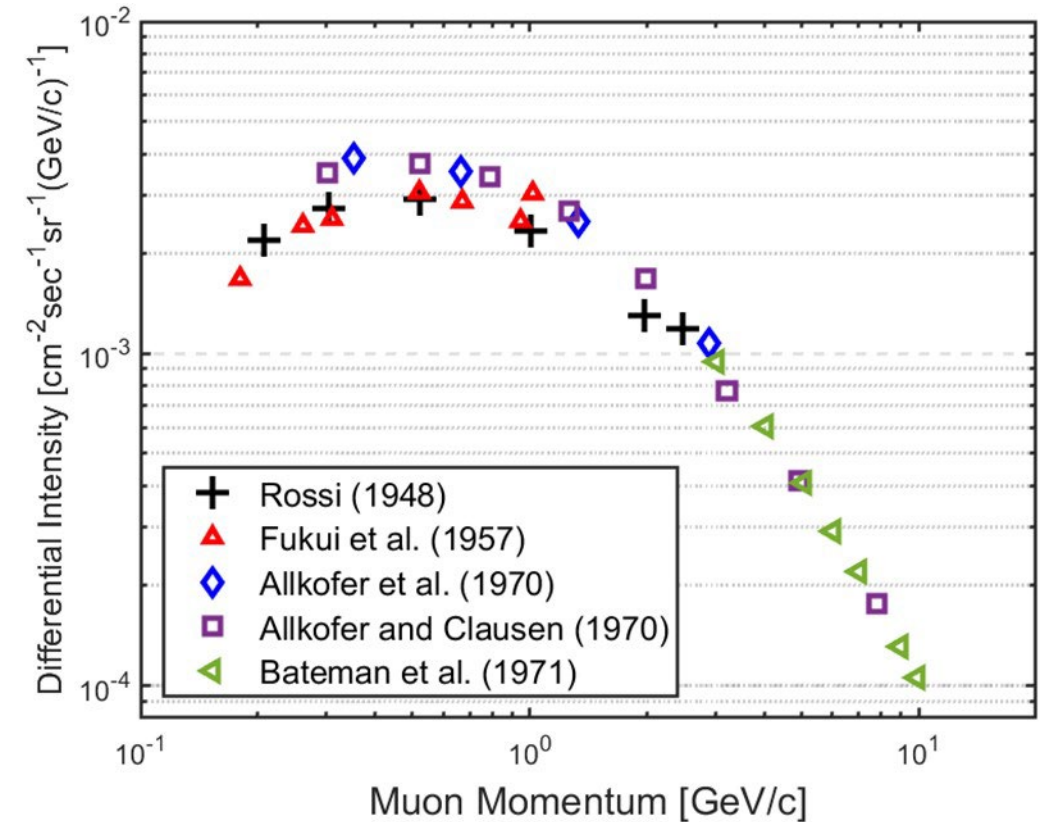


Fig. 1.1 Vertical differential cosmic momentum spectrum at sea level with zenith angle 0°

Grieder, P. K. F. (2001). Cosmic Rays at Earth. In Elsevier Science. Elsevier Science.

I. INTRODUCTION

2. Problem Statement

Importance of measuring muon momentum

$$\sigma_{\theta} = \frac{13.6 \text{ MeV}}{\beta c p} \sqrt{\frac{X}{X_0}} \left[1 + 0.088 \log_{10} \left(\frac{X}{X_0} \right) \right]$$

- σ_{θ} : standard deviation of scattering angle distribution
- $\beta c p$: product of cosmic muon velocity and momentum
- X/X_0 : Ratio of scattering length to radiation length

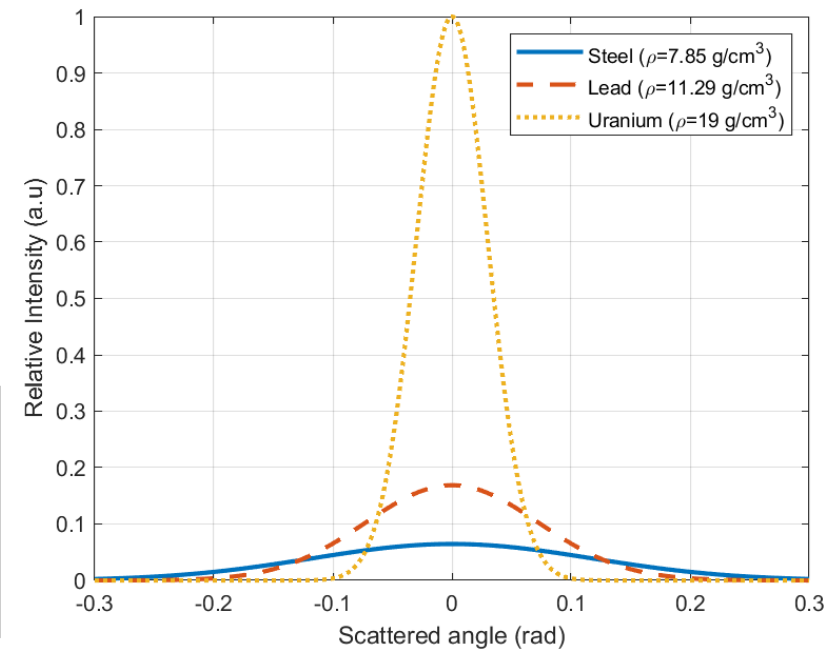
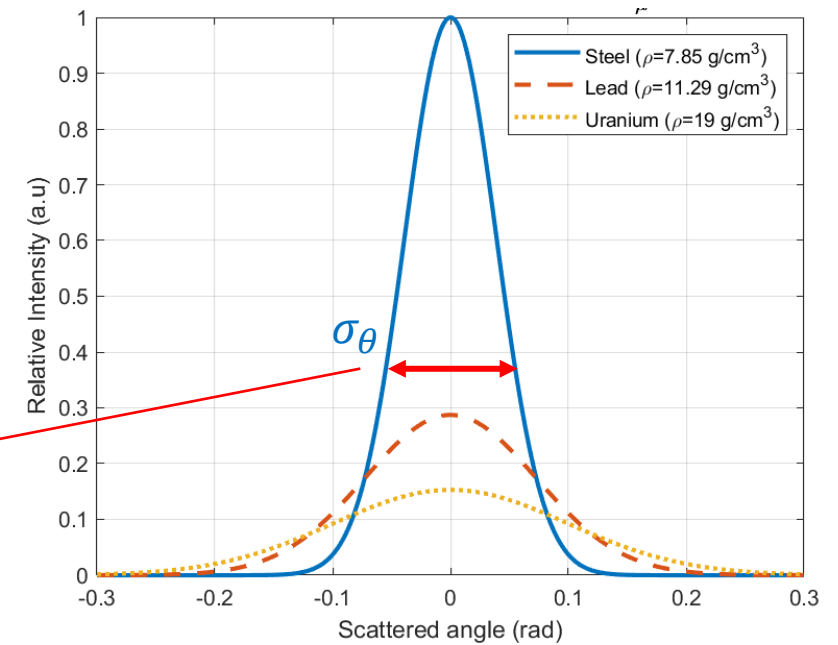


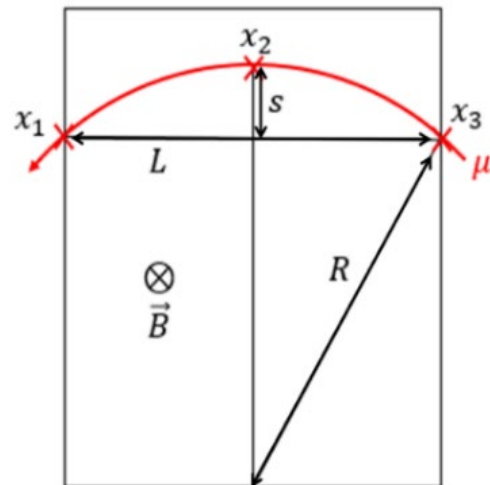
Fig. 1.2 Reconstructed Gaussian distributions for steel, lead, and uranium when muon momentum is 3 GeV/c (top) and 1, 3, and 10 GeV/c (bottom).

I. INTRODUCTION

2. Problem Statement

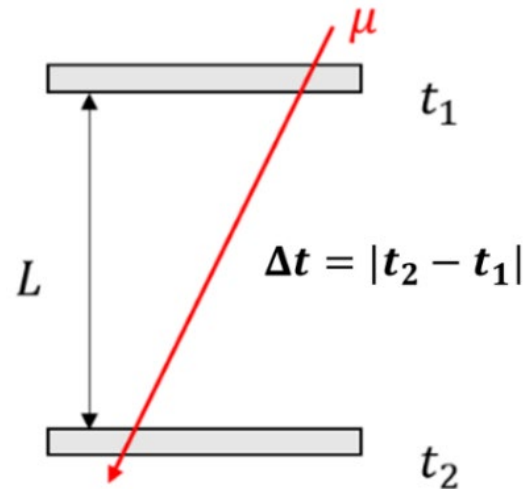
Three existing techniques to measure muon momentum

Magnets



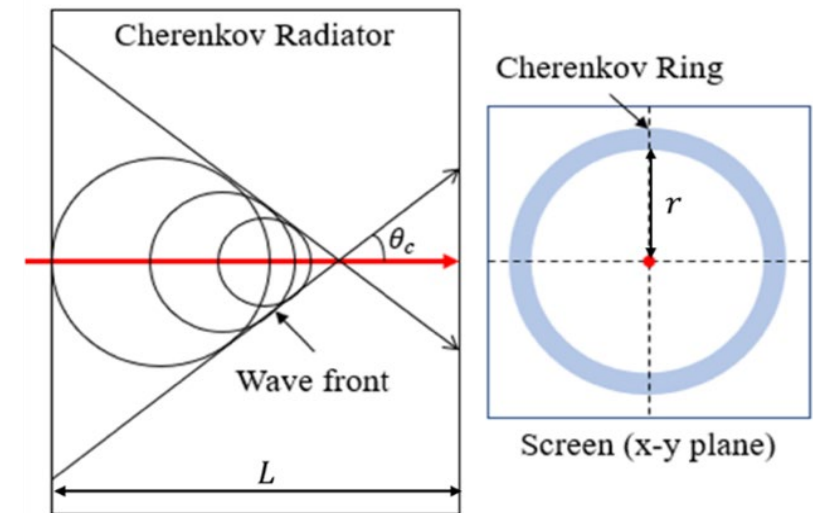
- High resolution
- Large and bulky magnets are required
- Impact the muon trajectory

Time of Flight



- Low resolution
- Long distance is required

Cherenkov Ring Imager



- High resolution
- Liquid radiator is required
- Array of optical sensors are required

I. INTRODUCTION

3. Research Objective

1. Development of fieldable muon spectrometer
 - * Requirements in design
 - Easily coupled with existing muon tomography system
 - Compact, portable, and light-weight
 - Compatible momentum measurement resolution
 - High accuracy
 - Preserve incoming and outgoing muon trajectories
2. Development of momentum-integrated imaging algorithm without increasing computational costs
3. Improvement in imaging resolution and reducing monitoring times in various muon applications

A Gas Cherenkov Muon Spectrometer for Nuclear Security Applications

TABLE OF CONTENTS

I. INTRODUCTION

1. Motivation
2. Problem Statement
3. Research Objective

II. MUON SPECTROMETER USING GAS CHERENKOV RADIATORS

1. Operational Principle
2. Optical Photon Emission
3. Results

III. MOMENTUM INTEGRATED IMAGING ALGORITHM

IV. MOMENTUM INTEGRATED MUON TOMOGRAPHY

1. Implementation of Cherenkov muon spectrometer in SNF monitoring
2. Results

V. SUMMARY AND CONCLUSION

II. MUON SPECTROMETER USING GAS CHERENKOV RADIATORS

1. Operational Principle

- Cherenkov Effect

$$\beta_{\mu} n > 1 \quad \text{Criterion for Cherenkov radiation}$$

$$p_{th} c = \frac{m_{\mu} c^2}{\sqrt{n^2 - 1}} \quad \text{Cherenkov threshold momentum, } p_{th}$$

- Lorentz-Lorenz Equation

$$n \approx \sqrt{1 + \frac{3A_m p}{RT}} \quad \text{Refractive index (} n \text{) of gas as a function of } p \text{ and } T$$

$$p_{th} c = m_{\mu} c^2 \sqrt{\frac{R T}{3A_m p}} \quad \text{Threshold momentum, } p_{th}, \text{ gas as a function of } p \text{ and } T$$

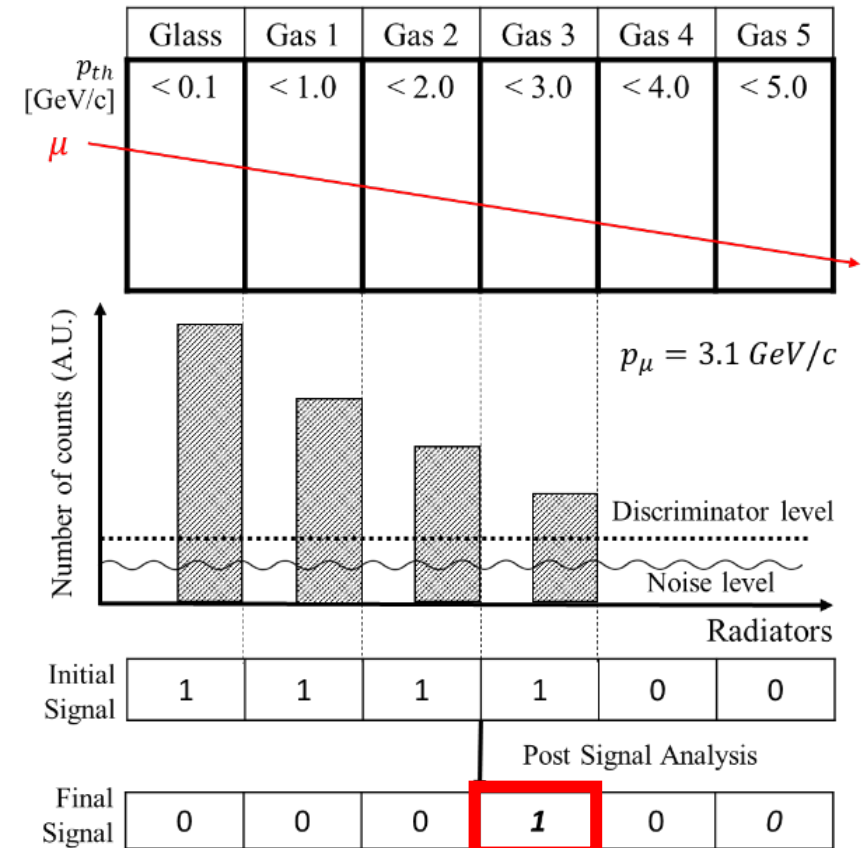


Fig. 2.1 Operational principle of Cherenkov muon spectrometer

II. MUON SPECTROMETER USING GAS CHERENKOV RADIATORS

1. Operational Principle

Prototype Design

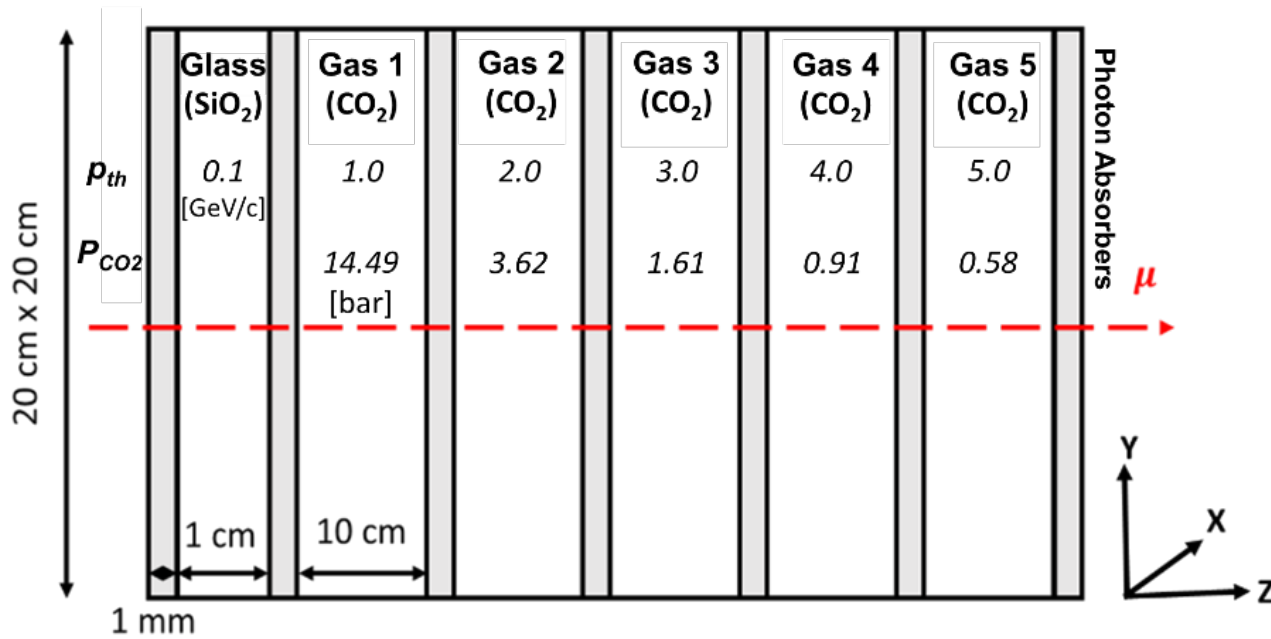


Fig. 2.2 Overview of Cherenkov muon spectrometer using one SiO₂ and five pressurized CO₂ radiators.

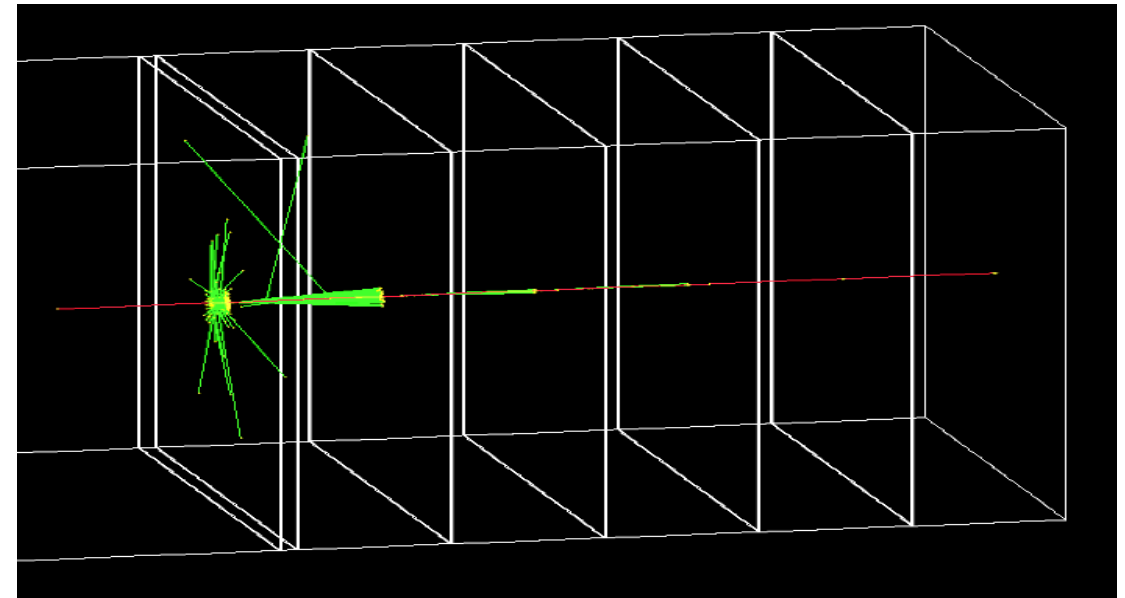
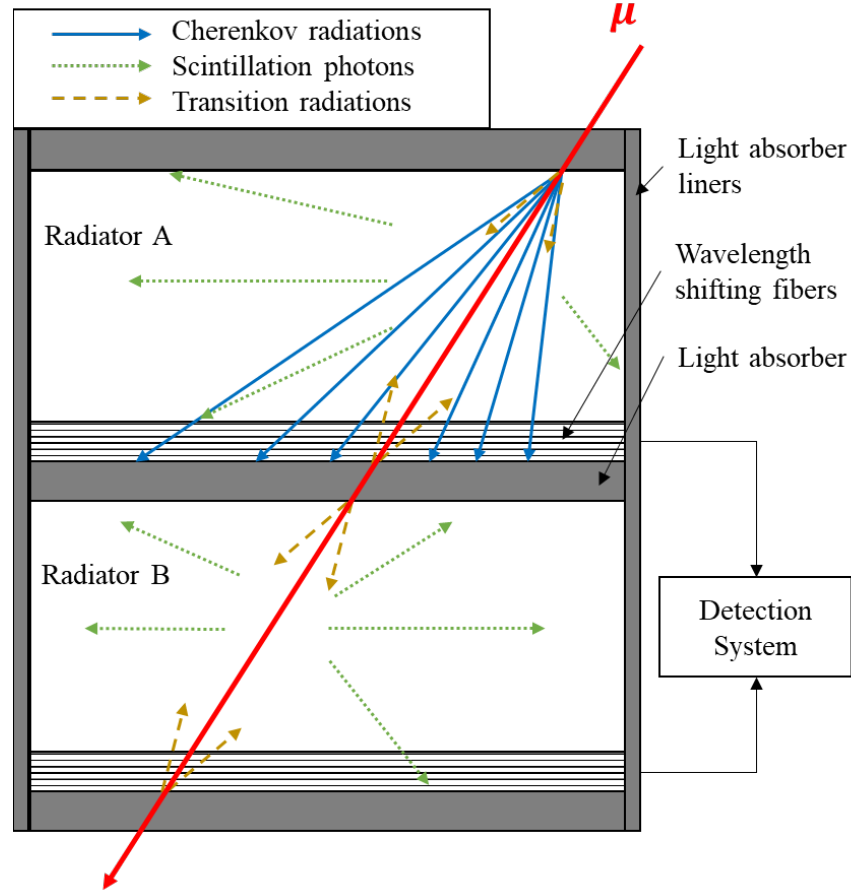


Fig. 2.3 Visualized Geant4 simulation when $p_{\mu} = 3.1$ GeV/c

II. MUON SPECTROMETER USING GAS CHERENKOV RADIATORS

2. Optical Photon Emission



1. Cherenkov radiation

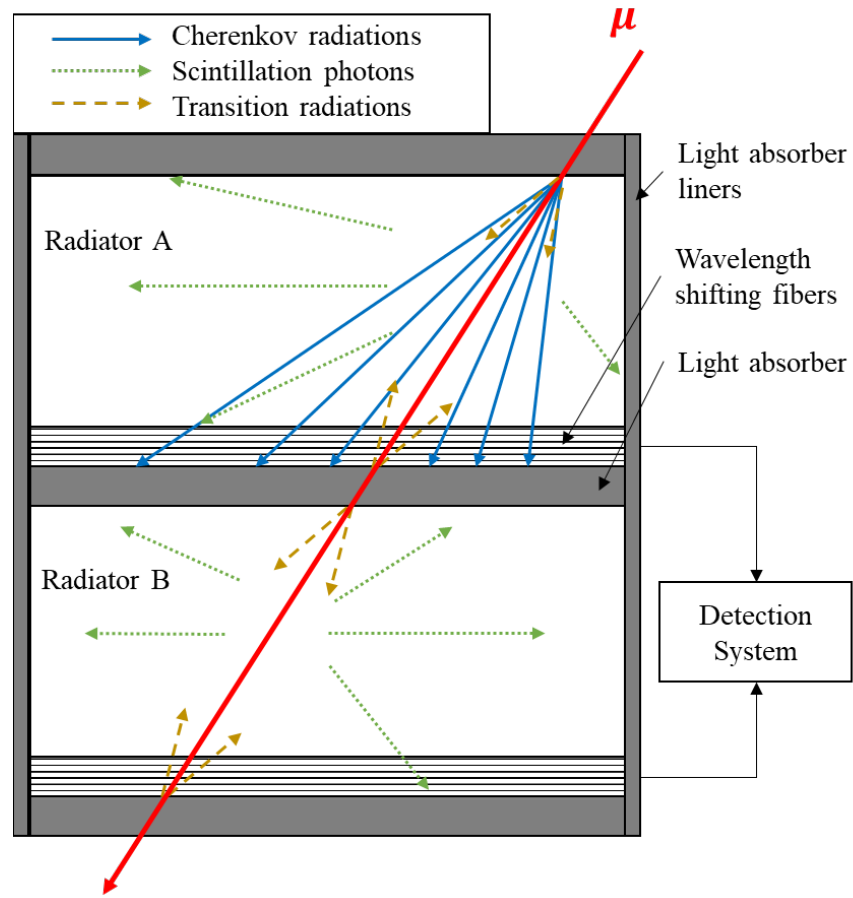
$$\frac{dN_{ch}}{dx} = 2\pi\alpha \int_{\lambda_1}^{\lambda_2} \left(1 - \frac{1}{n^2(\lambda)\beta^2} \right) \frac{d\lambda}{\lambda^2}$$

- dN_{ch}/dx : Light intensity of Cherenkov radiation in a unit length
- α : Fine structure constant
- n : Refractive index
- $\lambda_{1,2}$: Lower and upper limit of Cherenkov light wavelength

Fig. 2.4 Three optical photon emission mechanisms

II. MUON SPECTROMETER USING GAS CHERENKOV RADIATORS

2. Optical Photon Emission



2. Scintillation

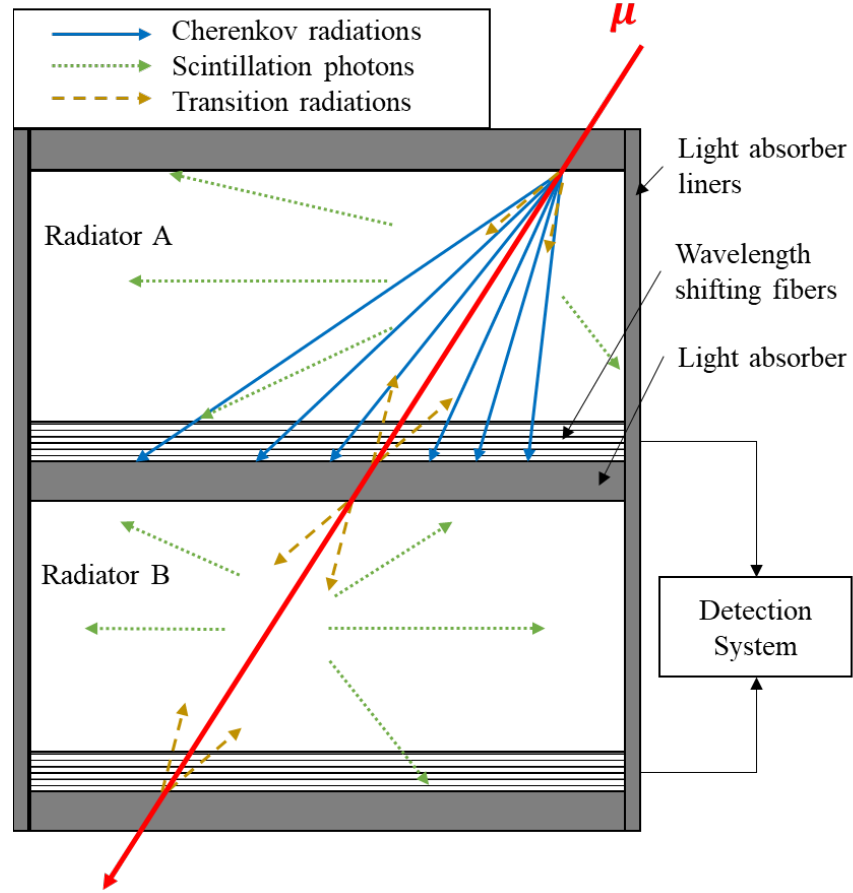
$$\frac{dN_{sc}}{dx} = S \frac{dE/dx}{1 + k_B(dE/dx)}$$

- dN_{sc}/dx : Light intensity of scintillation in a unit length
- dE/dx : Energy loss of muon in a unit length
- k_B : Birks' constant
- S : Scintillation efficiency

Fig. 2.4 Three optical photon emission mechanisms

II. MUON SPECTROMETER USING GAS CHERENKOV RADIATORS

2. Optical Photon Emission



3. Transition radiation

$$N_{tr} \Big|_{\text{per boundary}} = \frac{\alpha}{\pi} \left[(\ln \gamma - 1)^2 + \frac{\pi^2}{12} \right]$$

- N_{tr} : Light intensity of transition radiation.
- α : Fine structure constant
- γ : Lorentz factor ($= 1/\sqrt{1 - \beta^2}$)
- β ($\equiv v/c$): Particle velocity in terms of c (speed of light)

Fig. 2.4 Three optical photon emission mechanisms

II. MUON SPECTROMETER USING GAS CHERENKOV RADIATORS

2. Optical Photon Emission

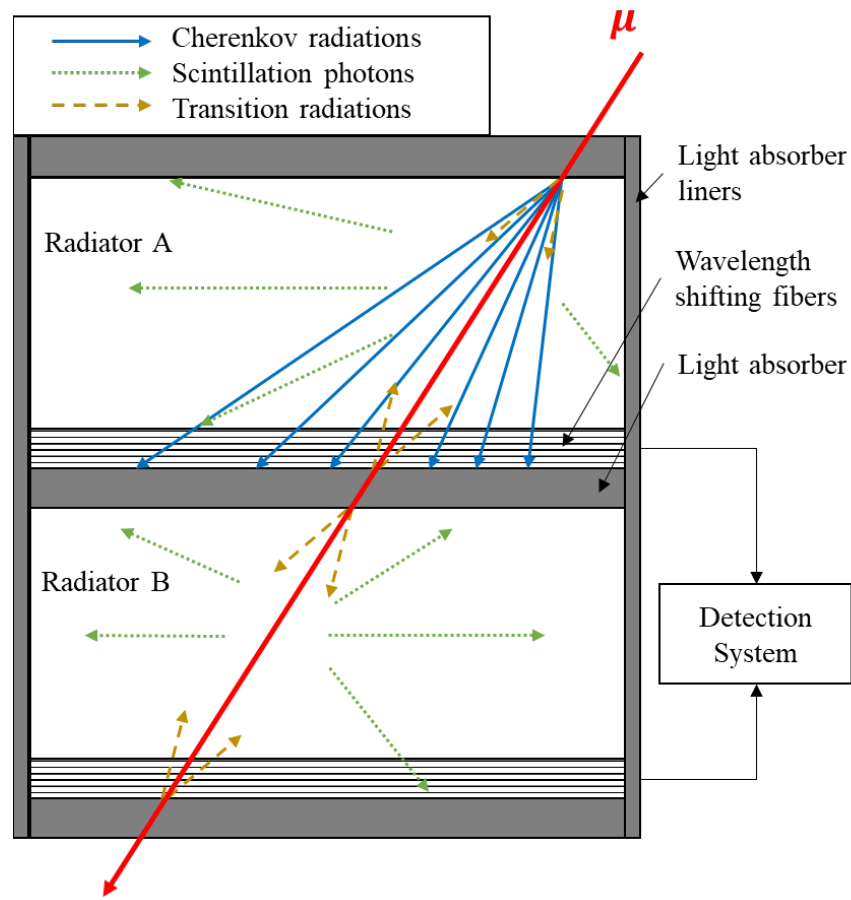


Fig. 2.4 Three optical photon emission mechanisms

4. Cherenkov radiation by secondary electrons, (1) μ decay
(2) $\mu \rightarrow e$ conversion

$$\mu^- \rightarrow e^- \bar{\nu}_e \nu_\mu$$

$$\mu^+ \rightarrow e^+ \nu_e \bar{\nu}_\mu$$

$$\mu N_{Al} \rightarrow e N_{Al}$$

$$p_{th,e} = \frac{m_e}{m_\mu} p_{th,\mu} \sim \frac{1}{207} p_{th,\mu}$$

- m_e : Rest mass of electron (~ 0.511 MeV/c)
- m_μ : Rest mass of muon (~ 105.66 MeV/c)
- $p_{th,\mu}$: Cherenkov threshold momentum for muons
- $p_{th,e}$: Cherenkov threshold momentum for electrons

II. MUON SPECTROMETER USING GAS CHERENKOV RADIATORS

2. Optical Photon Emission

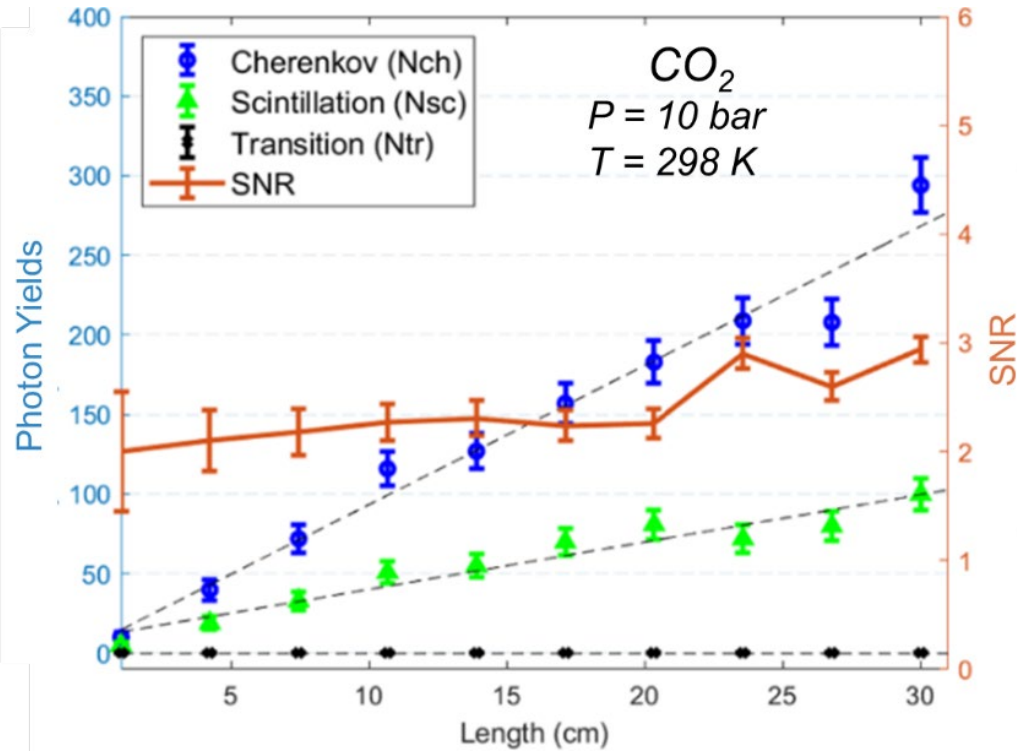


Fig. 2.5 Expected light yield by three optical photon emission mechanisms

1. Cherenkov radiation

$$\frac{dN_{ch}}{dx} = 2\pi\alpha \int_{\lambda_1}^{\lambda_2} \left(1 - \frac{1}{n^2(\lambda)\beta^2}\right) \frac{d\lambda}{\lambda^2}$$

2. Scintillation

$$\frac{dN_{sc}}{dx} = S \frac{dE/dx}{1 + k_B(dE/dx)}$$

3. Transition radiation

$$N_{tr} \Big|_{\text{per boundary}} = \frac{\alpha}{\pi} \left[(\ln \gamma - 1)^2 + \frac{\pi^2}{12} \right]$$

4. Cherenkov radiation

- due to secondary e-
(1) μ decay
(2) $\mu \rightarrow e$ conversion

$$\mu^- \rightarrow e^- \bar{\nu}_e \nu_\mu$$

$$\mu^+ \rightarrow e^+ \nu_e \bar{\nu}_\mu$$

$$\mu N_{Al} \rightarrow e N_{Al}$$

II. MUON SPECTROMETER USING GAS CHERENKOV RADIATORS

3. Results

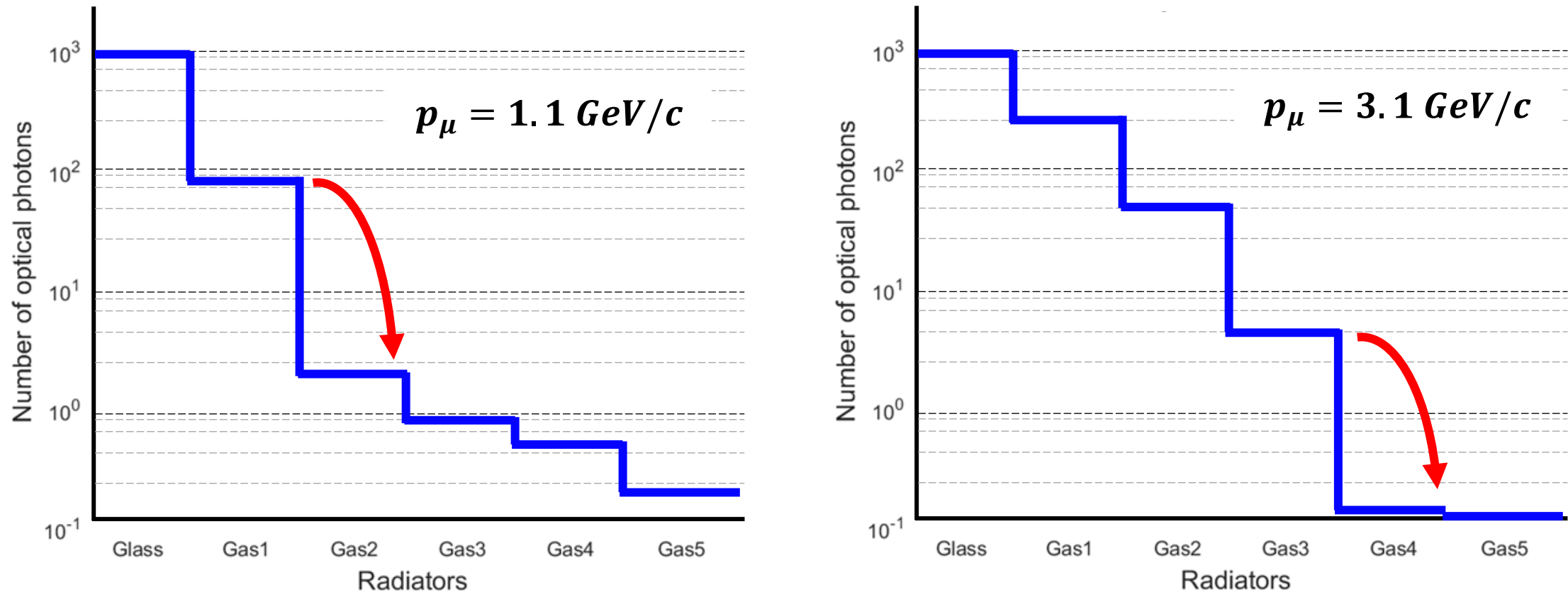


Fig. 2.6 Expected number of photon by Cherenkov radiation in each radiator when $p_\mu = 1.1$ (left) and $3.1 \text{ GeV}/c$ (right).

II. MUON SPECTROMETER USING GAS CHERENKOV RADIATORS

3. Results

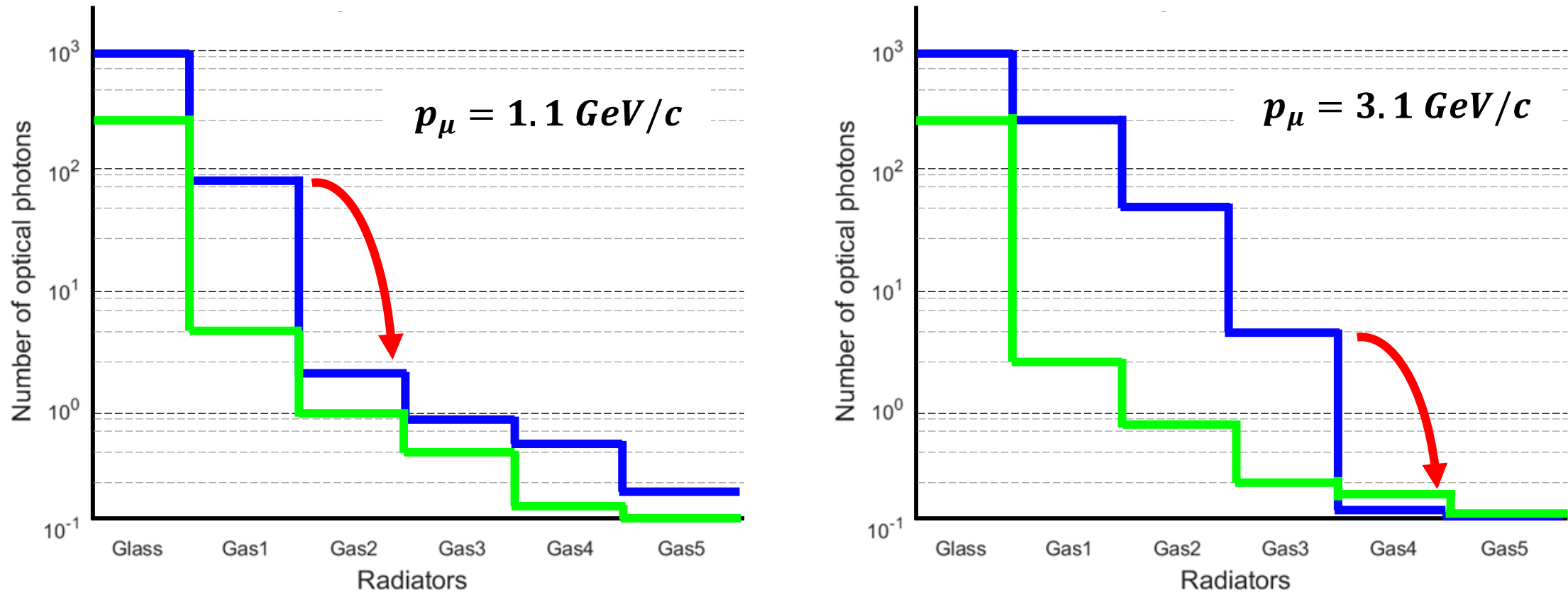
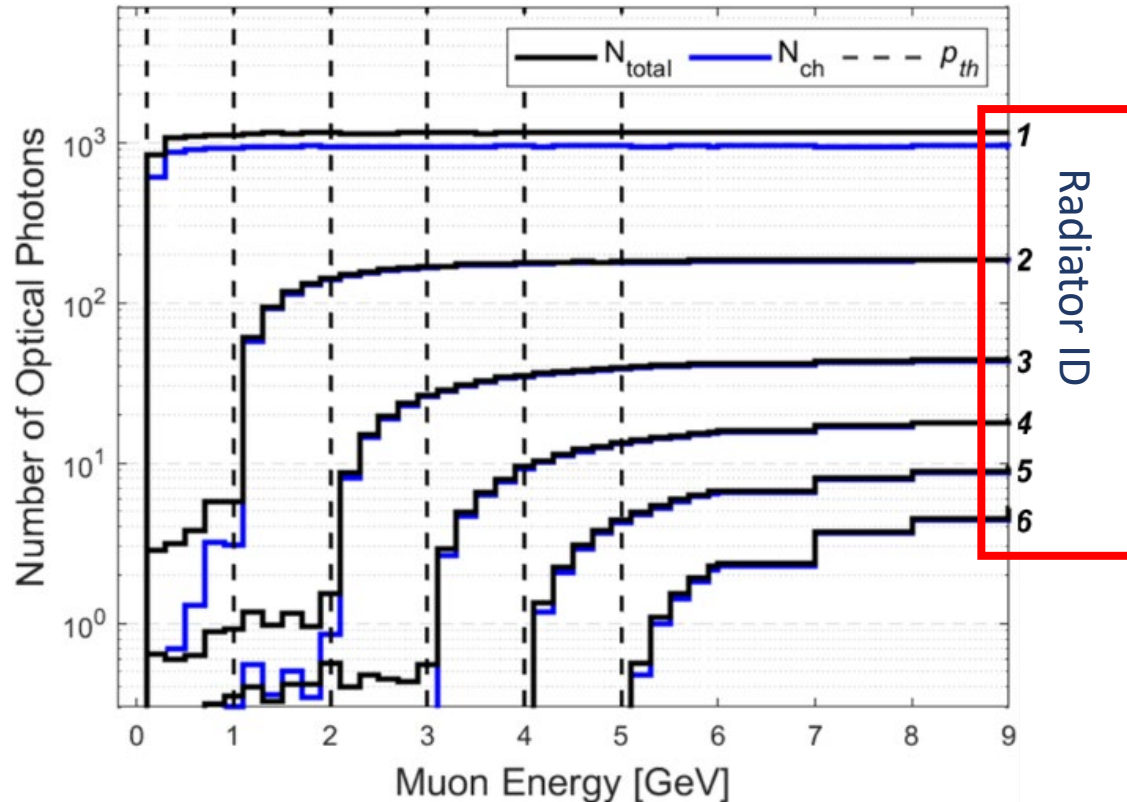


Fig. 2.7 Expected number of photon by Cherenkov radiation and scintillation in each radiator when $p_\mu = 1.1$ (left) and 3.1 GeV/c (right).

II. MUON SPECTROMETER USING GAS CHERENKOV RADIATORS

3. Results

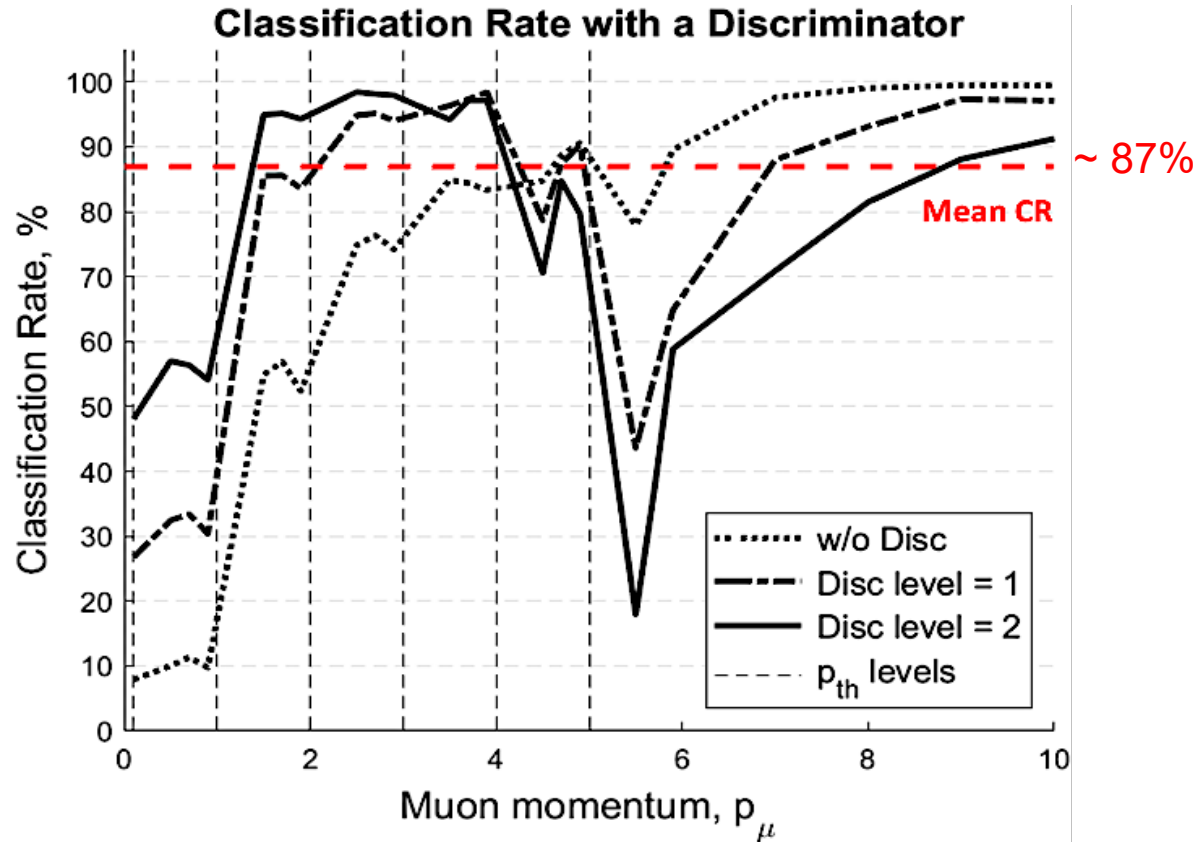


- Total number of optical photons provides clear signal (rapid increase) of muon momentum.
- The results demonstrate the feasibility of our Cherenkov muon spectrometer.

Fig. 2.8 Total Number of photons (Cherenkov radiation + Scintillation) as a function of $E\mu$ in each radiator

II. MUON SPECTROMETER USING GAS CHERENKOV RADIATORS

3. Results

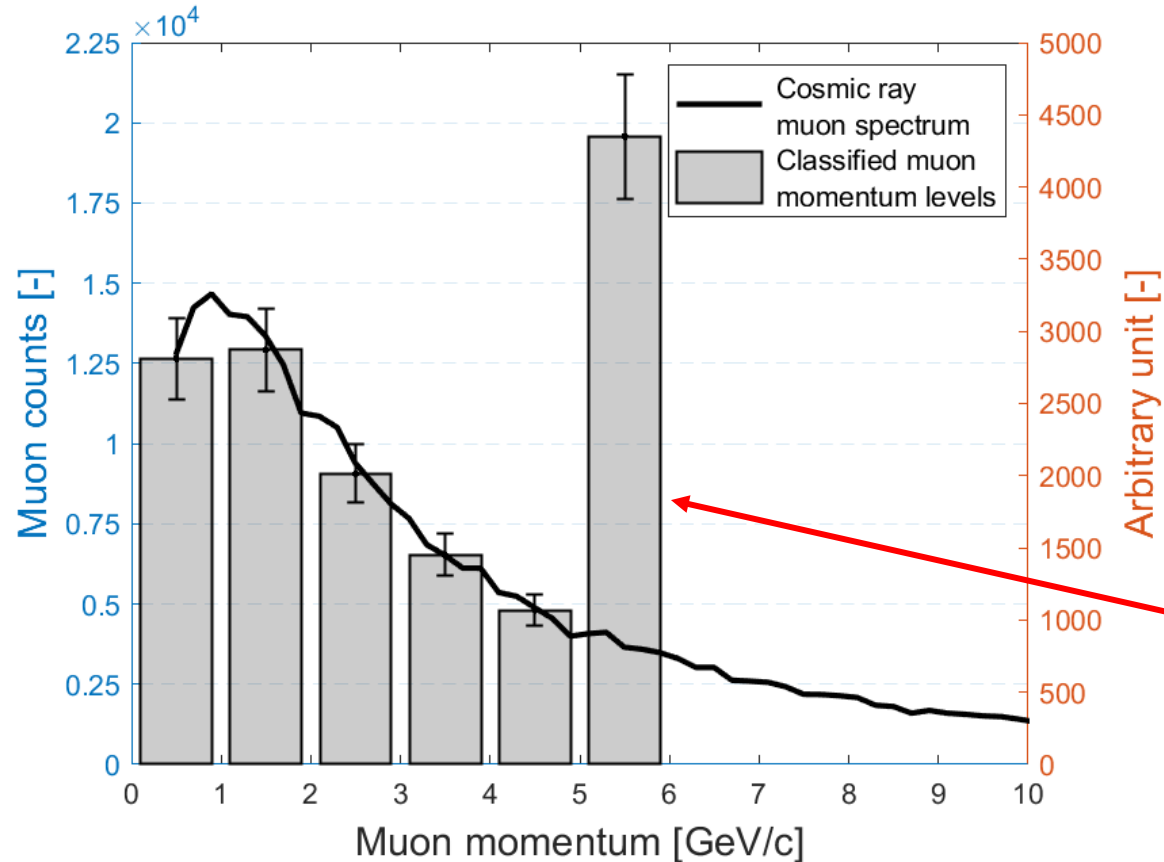


- $$CR = \frac{\text{True Positive Classification}}{\text{Positive Classification}}$$
- Discriminator uniformly deducts photon signals to eliminate noise.
 - By using a combination of various levels of discriminators, the mean CR is ~87%

Fig. 2.9 Classification as a function of muon momentum with various discriminator levels

II. MUON SPECTROMETER USING GAS CHERENKOV RADIATORS

3. Results

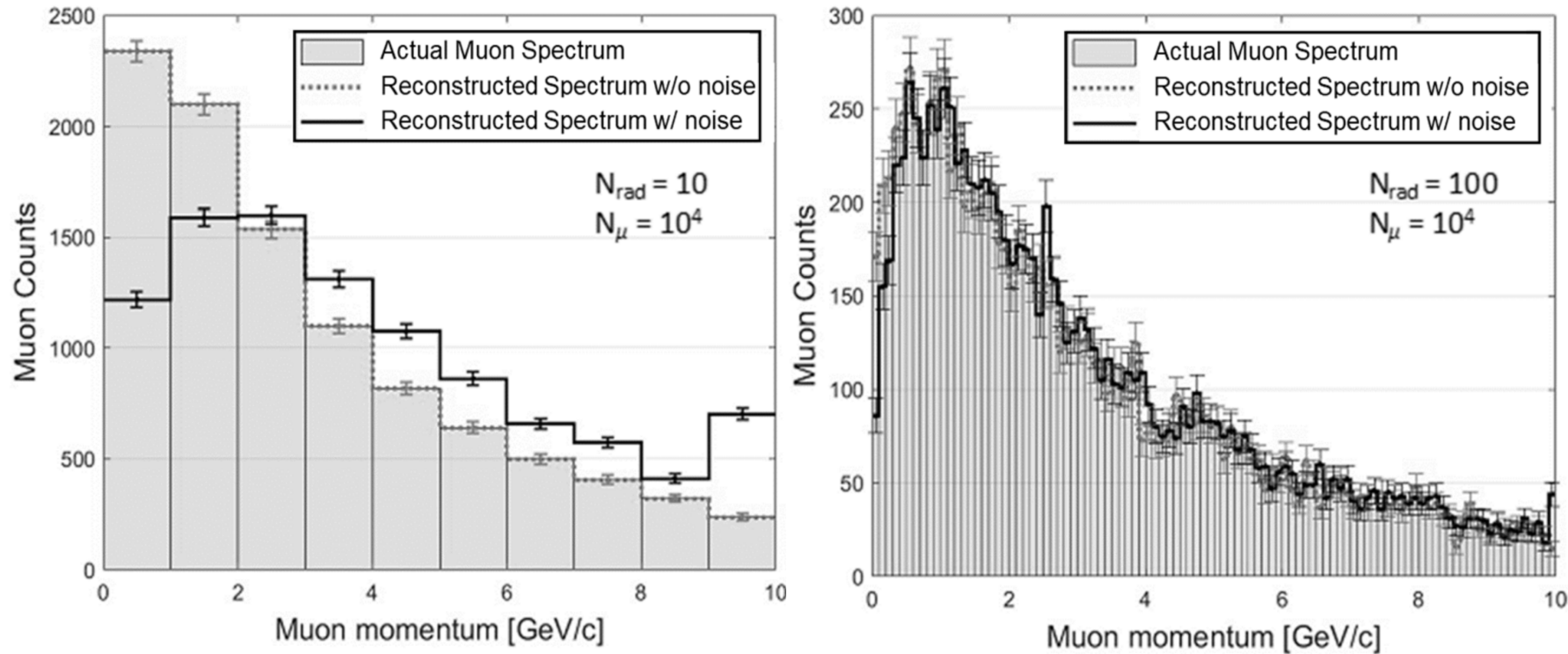


- Cosmic ray muon spectrum was successfully reconstructed using 6 radiators.
- All muons with $p_\mu > 5$ GeV/c are recorded and accumulated in the 6th bin.
- This problem can be easily resolved by increasing the number of radiators.

Fig. 2.10 Reconstructed cosmic ray muon spectrum using six radiators.

II. MUON SPECTROMETER USING GAS CHERENKOV RADIATORS

3. Results



- $N = 10$
- $\sigma_p = \pm 0.5 \text{ GeV}/c$
- $\sigma_p/p|_{\text{mean}} = 21.33 \%$

- $N = 100$
- $\sigma_p = \pm 0.05 \text{ GeV}/c$
- $\sigma_p/p|_{\text{mean}} = 3.35 \%$

Fig. 2.11 Reconstructed cosmic ray muon spectrum using extended number of radiators, 10 (left) and 100 (right)

A Gas Cherenkov Muon Spectrometer for Nuclear Security Applications

TABLE OF CONTENTS

- I. INTRODUCTION
 - 1. Motivation
 - 2. Problem Statement
 - 3. Research Objective
- II. MUON SPECTROMETER USING GAS CHERENKOV RADIATORS
 - 1. Operational Principle
 - 2. Optical Photon Emission
 - 3. Results
- III. **MOMENTUM INTEGRATED IMAGING ALGORITHM**
- IV. MOMENTUM INTEGRATED MUON TOMOGRAPHY
 - 1. Implementation of Cherenkov muon spectrometer in SNF monitoring
 - 2. Results
- V. SUMMARY AND CONCLUSION

III. MOMENTUM INTEGRATED IMAGING ALGORITHM

PoCA	mPoCA
<ol style="list-style-type: none"> 1. Voxlated the volume of interest. 2. Find a single scattering point using PoCA algorithm. $\rightarrow P_{PoCA} = [P_x, P_y, P_z]$ 	
<ol style="list-style-type: none"> 3a. Compute a scattering angle, θ. 4a. Record θ with P_{PoCA}. $\rightarrow V_{xyz} = [P_x, P_y, P_z, \theta]$ 5a. Plot θ at P_{PoCA}. 	<ol style="list-style-type: none"> 3b. Compute M-value. 4b. Record M with P_{PoCA}. $\rightarrow M_{xyz} = [P_x, P_y, P_z, M]$ 5b. Plot M at P_{PoCA}.

Fig. 3.1 Simplified pseudocodes for PoCA and mPoCA algorithms for muon scattering tomography

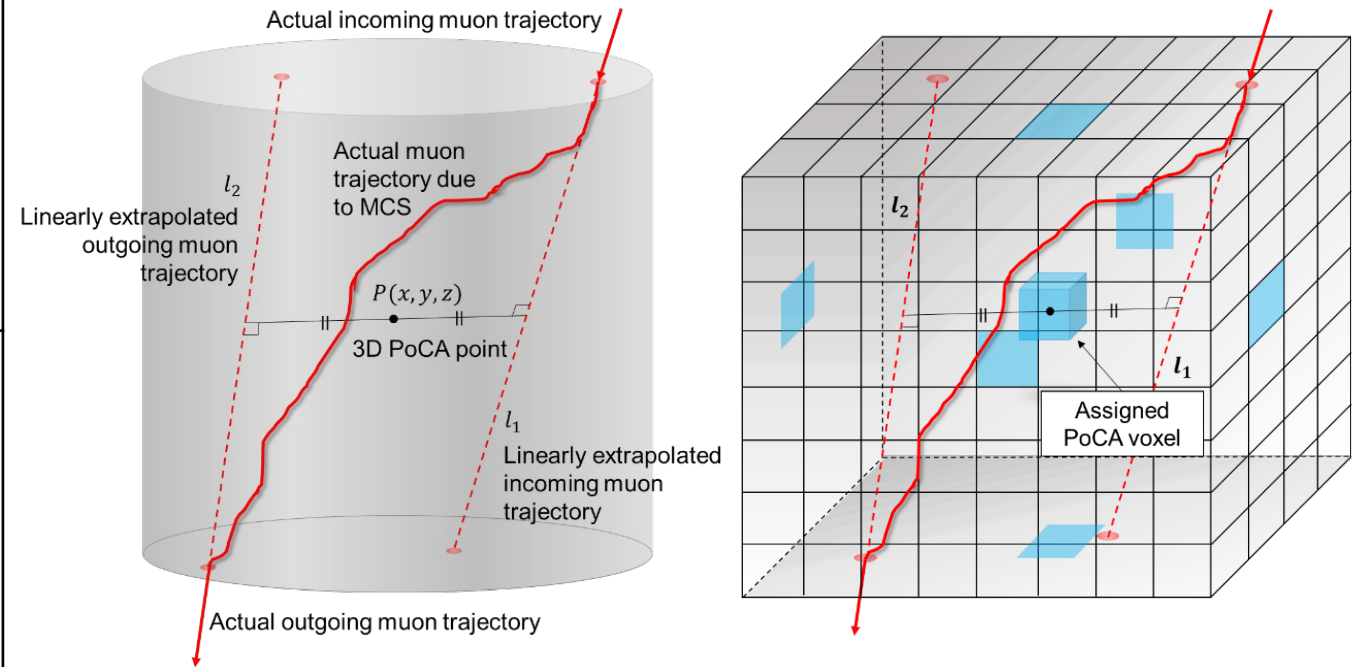


Fig. 3.2 Point of Closest Approach (PoCA) and voxelated volume of interest

III. MOMENTUM INTEGRATED IMAGING ALGORITHM

PoCA	mPoCA
<ol style="list-style-type: none"> Voxelate the volume of interest. Find a single scattering point using PoCA algorithm. $\rightarrow P_{PoCA} = [P_x, P_y, P_z]$ 	
<p>3a. Compute a scattering angle, θ.</p> <ol style="list-style-type: none"> Record θ with P_{PoCA}. $\rightarrow V_{xyz} = [P_x, P_y, P_z, \theta]$ Plot θ at P_{PoCA}. 	<ol style="list-style-type: none"> Compute M-value. Record M with P_{PoCA}. $\rightarrow M_{xyz} = [P_x, P_y, P_z, M]$ Plot M at P_{PoCA}.

Fig. 3.1 Simplified pseudocodes for PoCA and mPoCA algorithms for muon scattering tomography

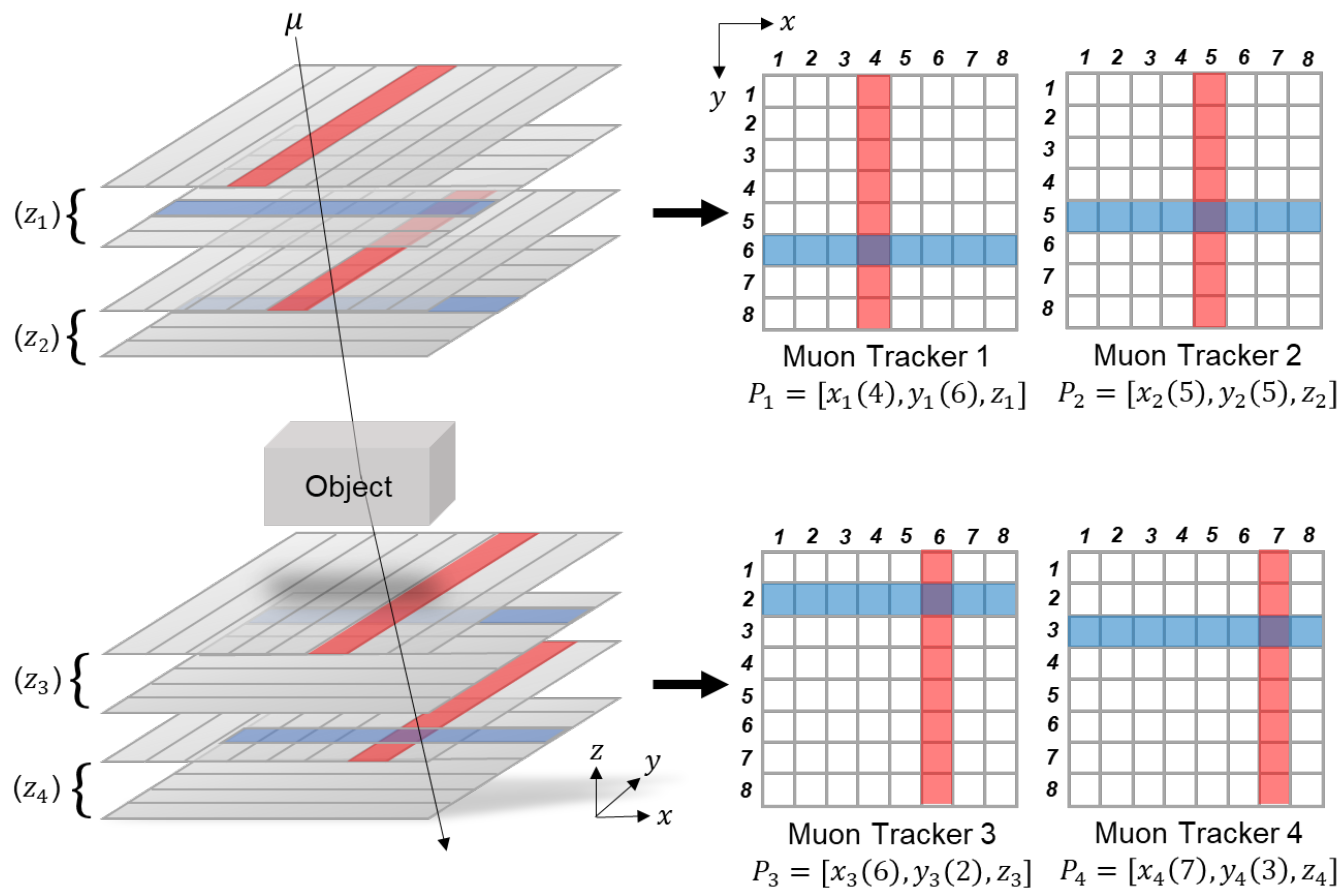


Fig. 3.3 Reconstruction of incoming and outgoing muon trajectories.

III. MOMENTUM INTEGRATED IMAGING ALGORITHM

PoCA	mPoCA
<ol style="list-style-type: none"> 1. Voxelize the volume of interest. 2. Find a single scattering point using PoCA algorithm. $\rightarrow P_{PoCA} = [P_x, P_y, P_z]$ 	
<ol style="list-style-type: none"> 3a. Compute a scattering angle, θ. 4a. Record θ with P_{PoCA}. $\rightarrow V_{xyz} = [P_x, P_y, P_z, \theta]$ 5a. Plot θ at P_{PoCA}. 	<ol style="list-style-type: none"> 3b. Compute M-value. 4b. Record M with P_{PoCA}. $\rightarrow M_{xyz} = [P_x, P_y, P_z, M]$ 5b. Plot M at P_{PoCA}.

Fig. 3.1 Simplified pseudocodes for PoCA and mPoCA algorithms for muon scattering tomography

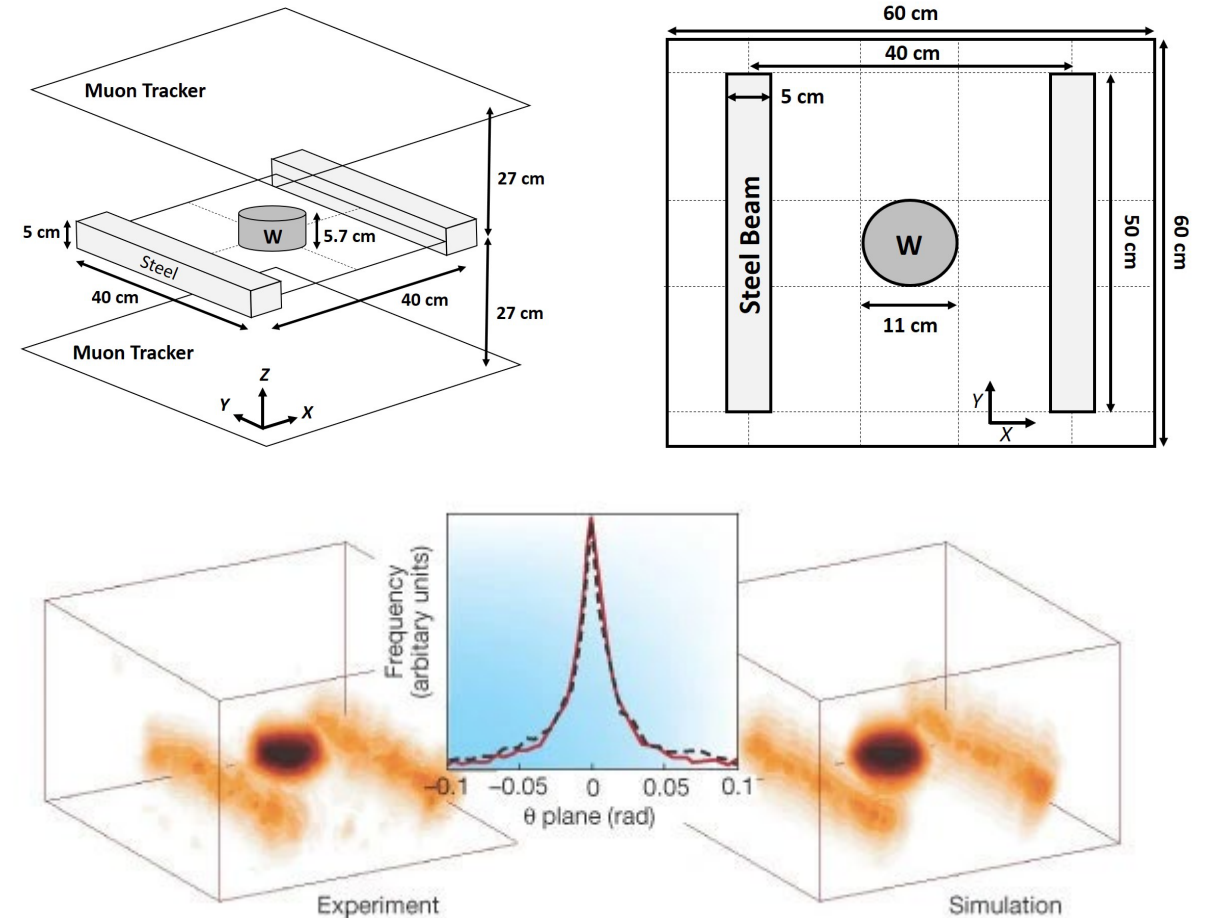


Fig. 3.4 Benchmarking experiment and simulation results by K. N. Borozdin et al.

III. MOMENTUM INTEGRATED IMAGING ALGORITHM

PoCA	mPoCA
<ol style="list-style-type: none"> 1. Voxelize the volume of interest. 2. Find a single scattering point using PoCA algorithm. $\rightarrow P_{PoCA} = [P_x, P_y, P_z]$ 	
<ol style="list-style-type: none"> 3a. Compute a scattering angle, θ. 4a. Record θ with P_{PoCA}. $\rightarrow V_{xyz} = [P_x, P_y, P_z, \theta]$ 5a. Plot θ at P_{PoCA}. 	<ol style="list-style-type: none"> 3b. Compute M-value. 4b. Record M with P_{PoCA}. $\rightarrow M_{xyz} = [P_x, P_y, P_z, M]$ 5b. Plot M at P_{PoCA}.

Fig. 3.1 Simplified pseudocodes for PoCA and mPoCA algorithms for muon scattering tomography

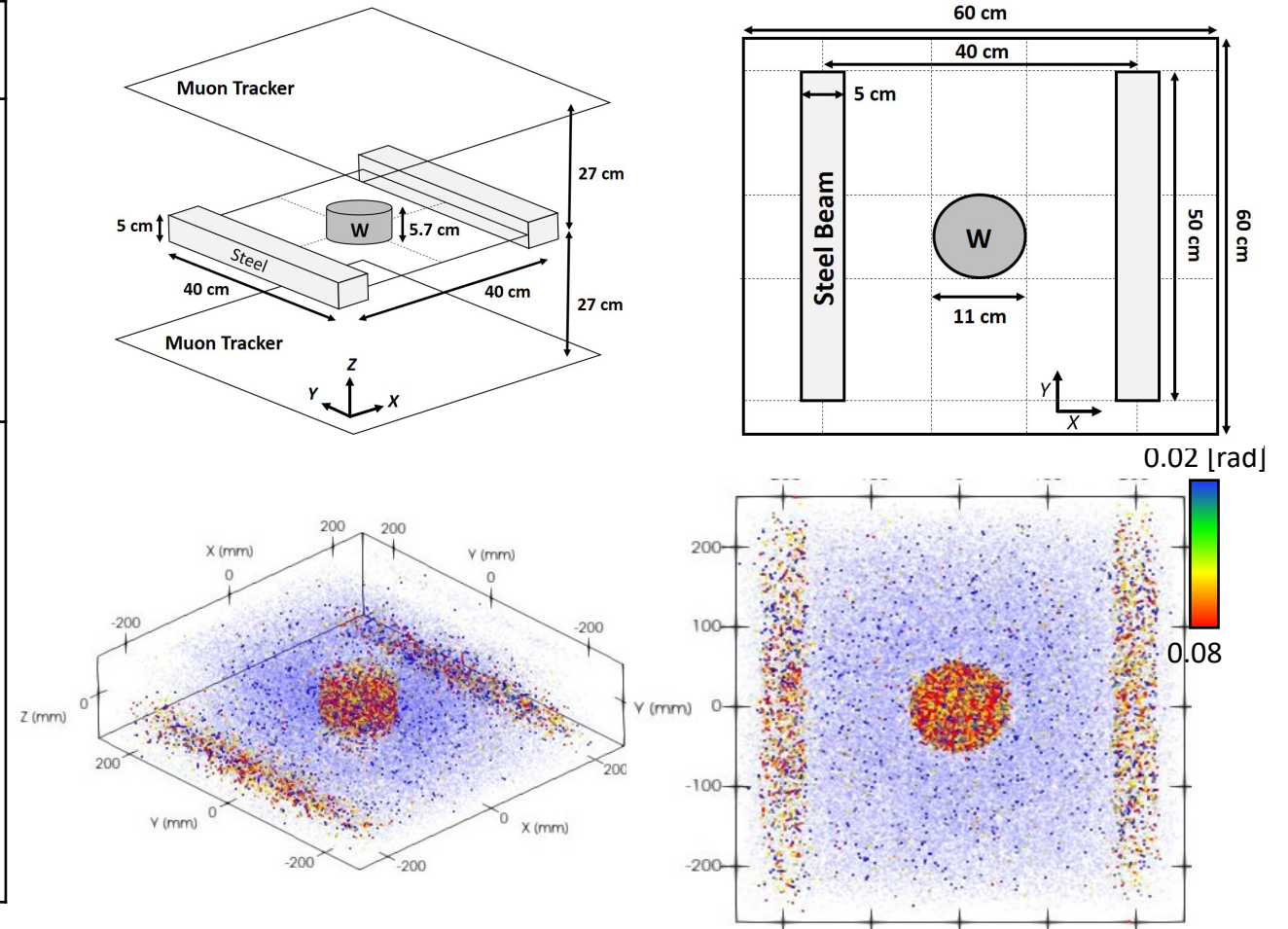
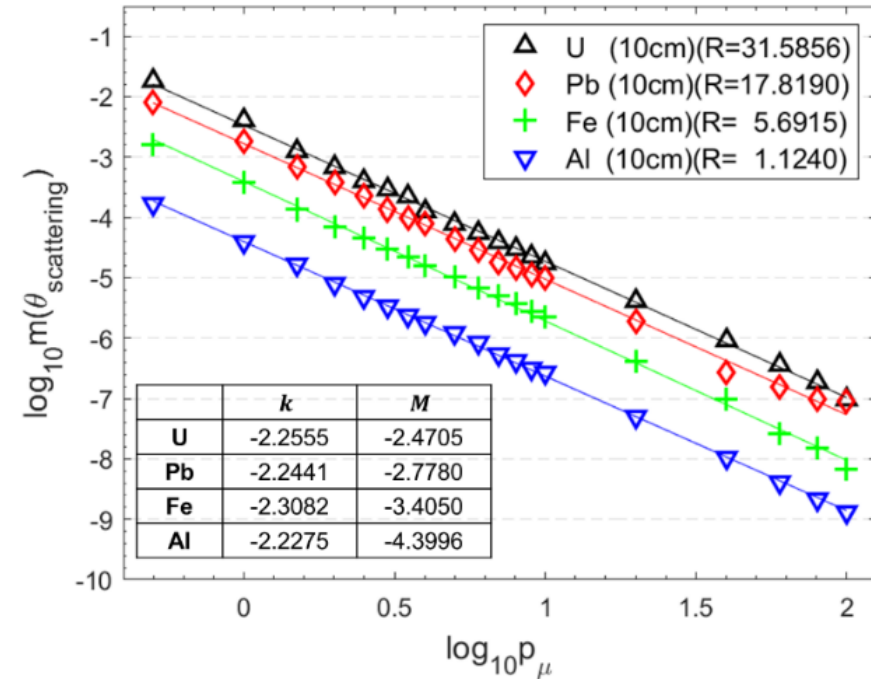


Fig. 3.4 Benchmarking experiment and simulation results by K. N. Borozdin et al.

III. MOMENTUM INTEGRATED IMAGING ALGORITHM

PoCA	mPoCA
<ol style="list-style-type: none"> Voxelize the volume of interest. Find a single scattering point using PoCA algorithm. $\rightarrow P_{PoCA} = [P_x, P_y, P_z]$ 	
<ol style="list-style-type: none"> 3a. Compute a scattering angle, θ. 4a. Record θ with P_{PoCA}. $\rightarrow V_{xyz} = [P_x, P_y, P_z, \theta]$ 5a. Plot θ at P_{PoCA}. 	<ol style="list-style-type: none"> 3b. Compute M-value. 4b. Record M with P_{PoCA}. $\rightarrow M_{xyz} = [P_x, P_y, P_z, M]$ 5b. Plot M at P_{PoCA}.

Fig. 3.1 Simplified pseudocodes for PoCA and mPoCA algorithms for muon scattering tomography



$$\log_{10} \text{mod}(\theta) = k \log_{10} p + M$$

$$M = \log_{10}(\theta [\text{rad}] \times p [\text{GeV}/c]^{2.24})$$

Fig. 3.5 Correlation between $\log_{10} \text{mod}(\theta)$ and $\log_{10} p$

III. MOMENTUM INTEGRATED IMAGING ALGORITHM

PoCA	mPoCA
<ol style="list-style-type: none"> 1. Voxelize the volume of interest. 2. Find a single scattering point using PoCA algorithm. $\rightarrow P_{PoCA} = [P_x, P_y, P_z]$ 	
<ol style="list-style-type: none"> 3a. Compute a scattering angle, θ. 4a. Record θ with P_{PoCA}. $\rightarrow V_{xyz} = [P_x, P_y, P_z, \theta]$ 5a. Plot θ at P_{PoCA}. 	<ol style="list-style-type: none"> 3b. Compute M-value. $\rightarrow M_{xyz} = [P_x, P_y, P_z, M]$ 4b. Record M with P_{PoCA}. 5b. Plot M at P_{PoCA}.

Fig. 3.1 Simplified pseudocodes for PoCA and mPoCA algorithms for muon scattering tomography

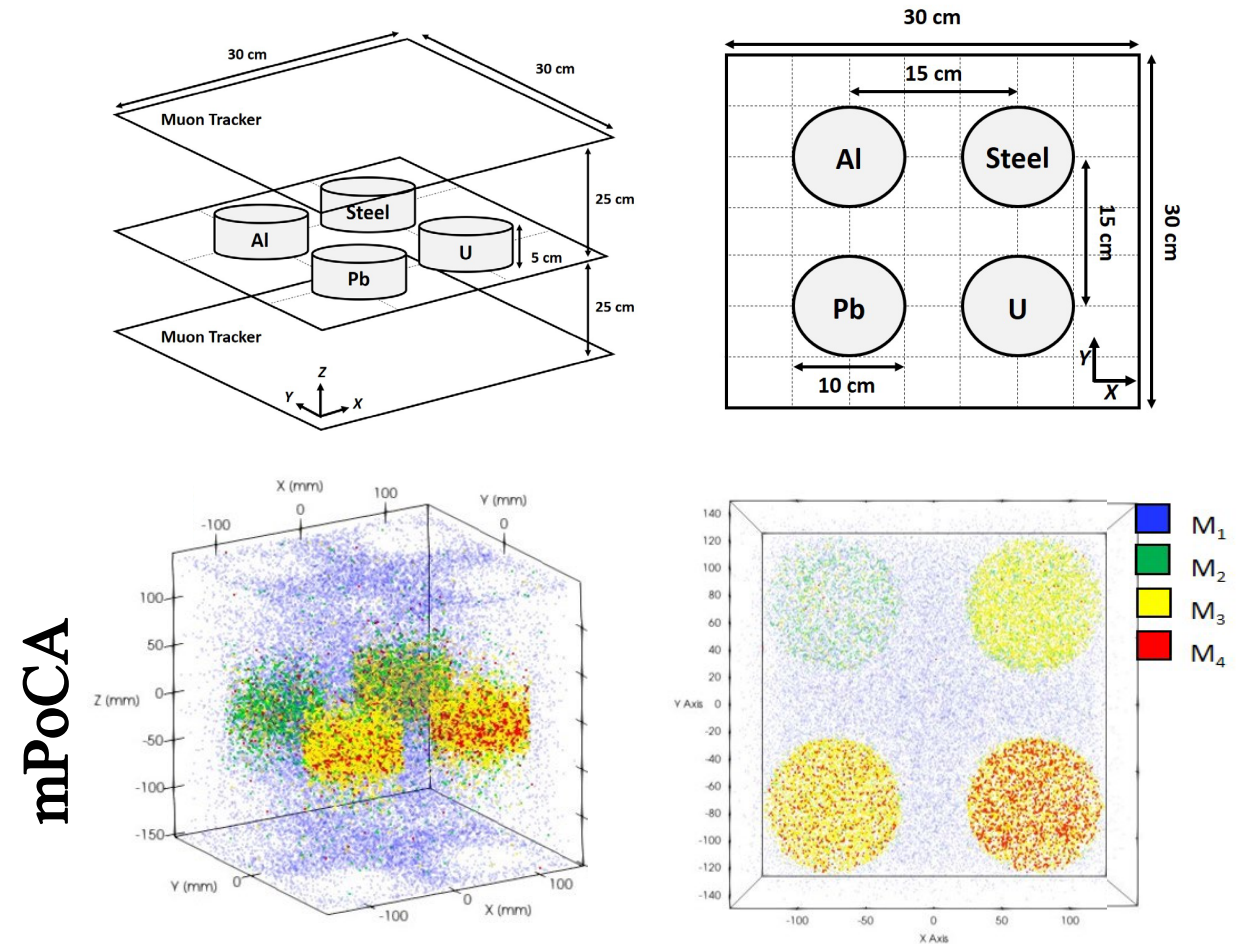


Fig. 3.6 Muon scattering tomography using mPoCA algorithm for aluminum, steel, lead, and uranium ³³

III. MOMENTUM INTEGRATED IMAGING ALGORITHM

PoCA	mPoCA
<ol style="list-style-type: none"> 1. Voxelize the volume of interest. 2. Find a single scattering point using PoCA algorithm. $\rightarrow P_{PoCA} = [P_x, P_y, P_z]$ 	
<ol style="list-style-type: none"> 3a. Compute a scattering angle, θ. 4a. Record θ with P_{PoCA}. $\rightarrow V_{xyz} = [P_x, P_y, P_z, \theta]$ 5a. Plot θ at P_{PoCA}. 	<ol style="list-style-type: none"> 3b. Compute M-value. $\rightarrow M_{xyz} = [P_x, P_y, P_z, M]$ 4b. Record M with P_{PoCA}. 5b. Plot M at P_{PoCA}.

Fig. 3.1 Simplified pseudocodes for PoCA and mPoCA algorithms for muon scattering tomography

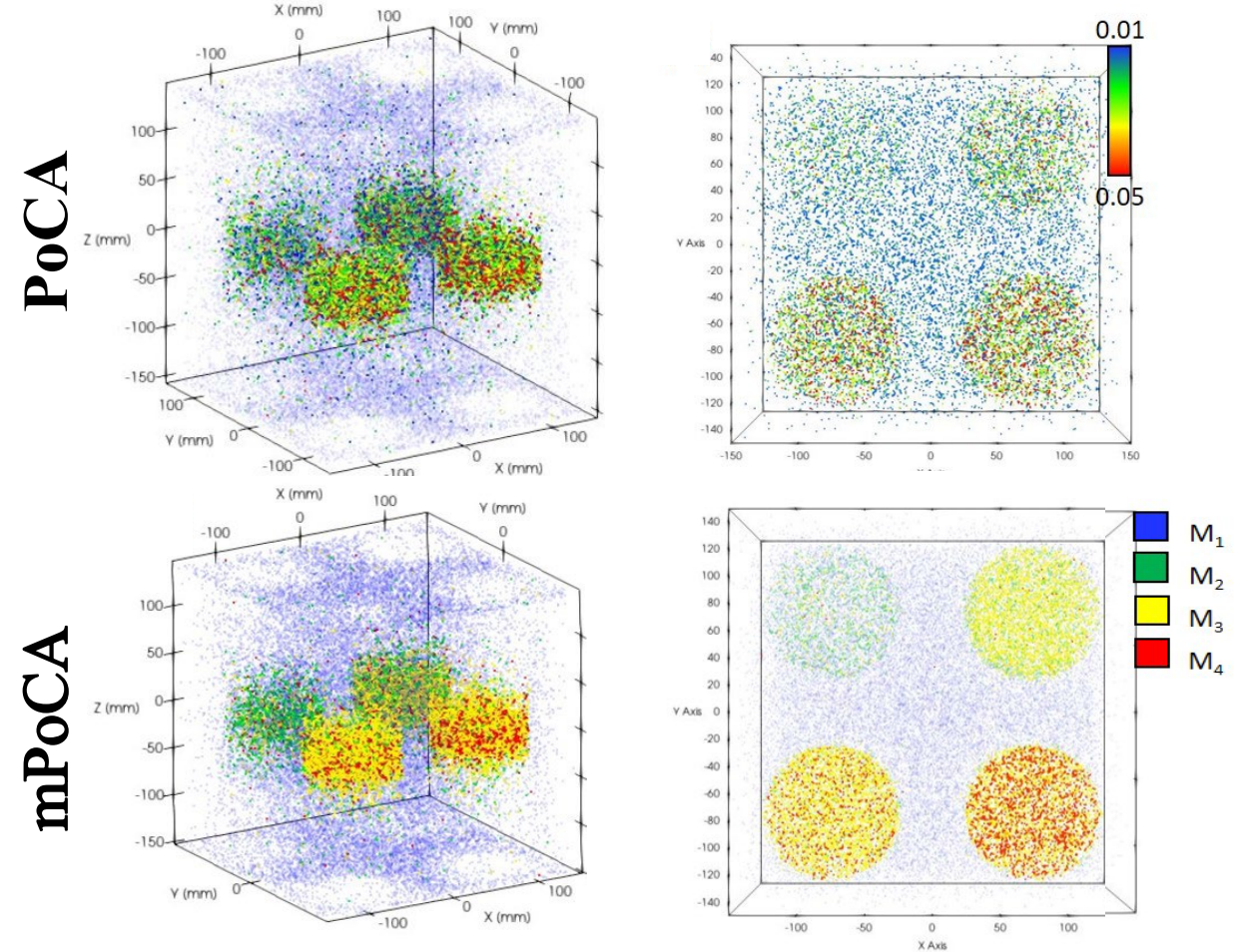


Fig. 3.7 PoCA and mPoCA algorithms for imaging aluminum, steel, lead, and uranium

A Gas Cherenkov Muon Spectrometer for Nuclear Security Applications

TABLE OF CONTENTS

- I. INTRODUCTION
 - 1. Motivation
 - 2. Problem Statement
 - 3. Research Objective
- II. MUON SPECTROMETER USING GAS CHERENKOV RADIATORS
 - 1. Operational Principle
 - 2. Optical Photon Emission
 - 3. Results
- III. MOMENTUM INTEGRATED IMAGING ALGORITHM
- IV. MOMENTUM INTEGRATED MUON TOMOGRAPHY**
 - 1. Implementation of Cherenkov muon spectrometer in SNF monitoring
 - 2. Results
- V. SUMMARY AND CONCLUSION

IV. MOMENTUM INTEGRATED MUON TOMOGRAPHY

1. Implementation of Cherenkov muon spectrometer in SNF monitoring

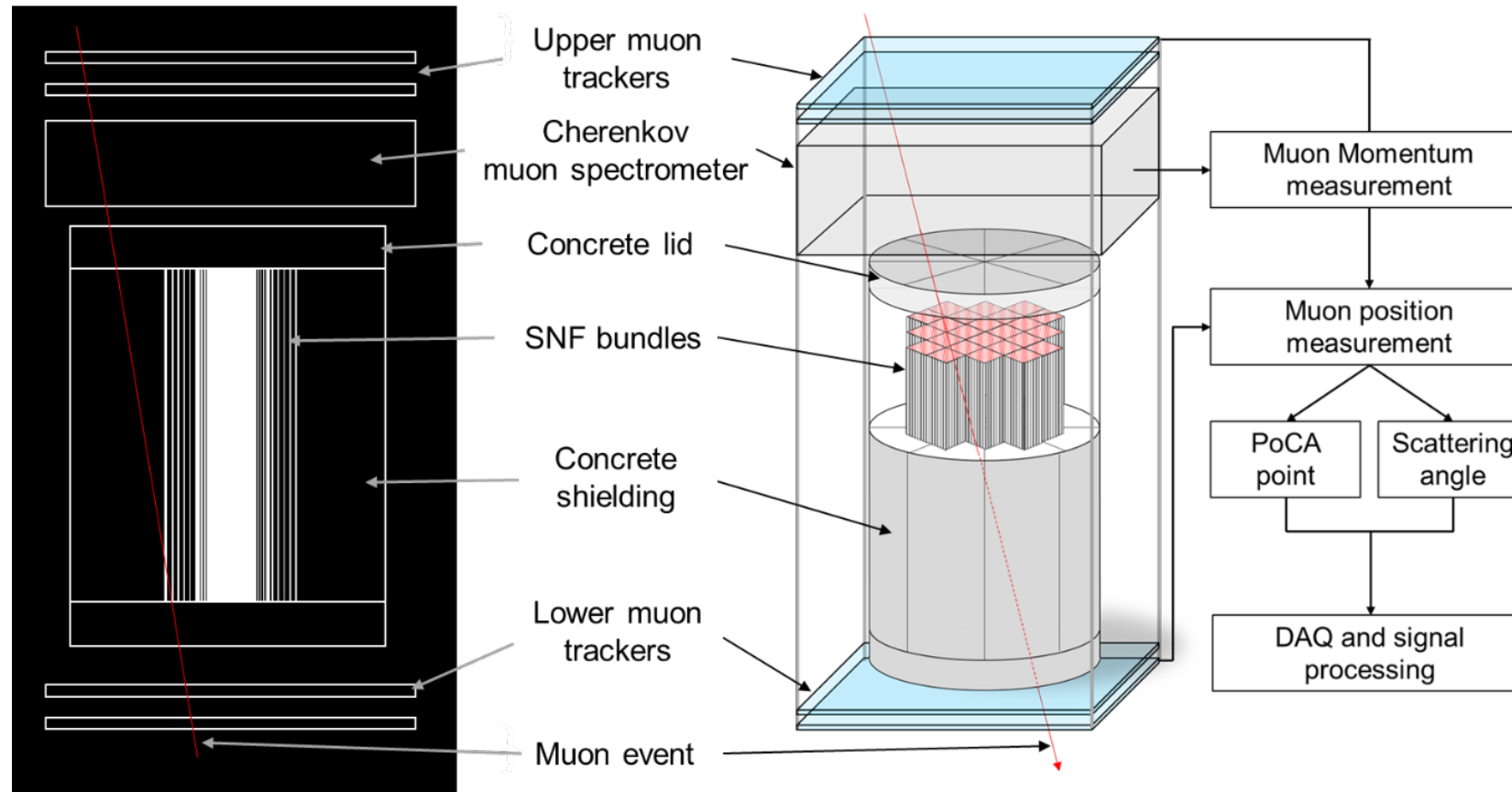


Fig. 4.1 Overview of the momentum integrated muon tomography system using the Cherenkov muon spectrometer for SNF dry cask imaging (right) and the visualized Geant4 model (left).

IV. MOMENTUM INTEGRATED MUON TOMOGRAPHY

2. Results

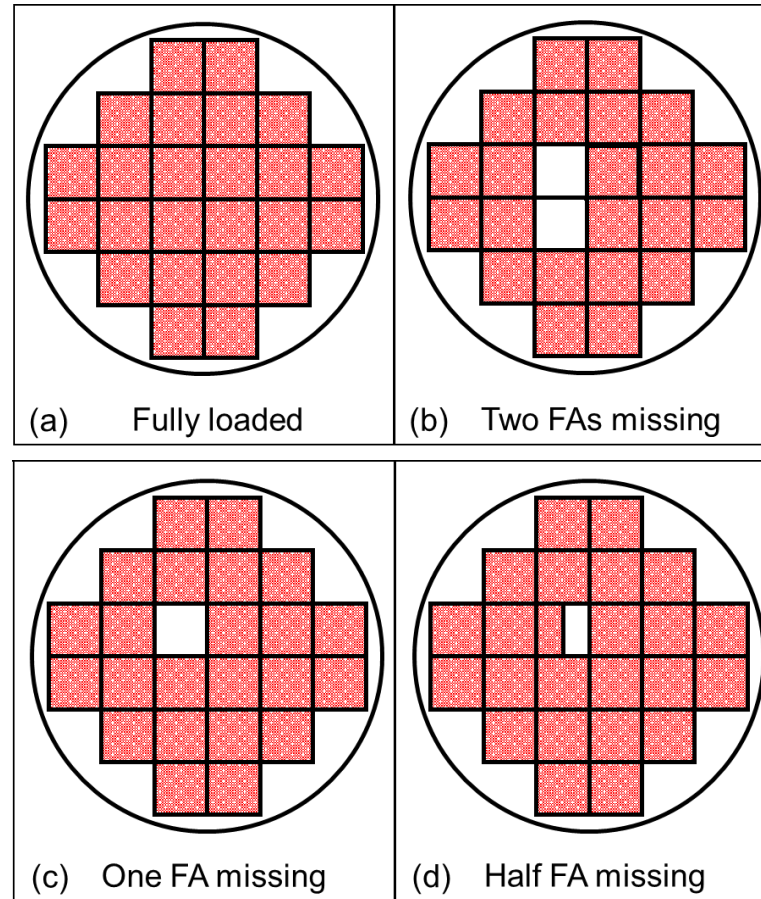
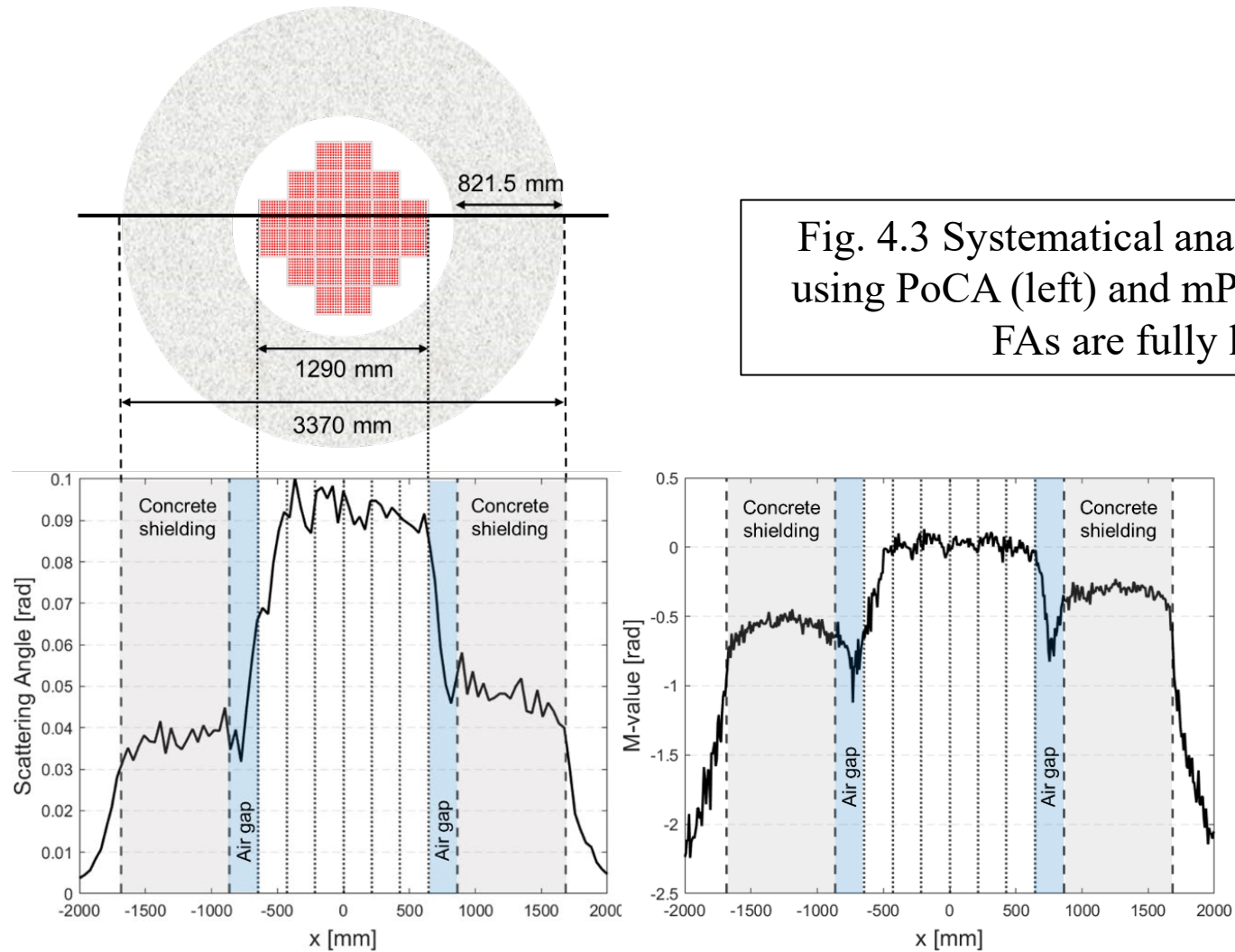


Fig. 4.2 Overview of four scenarios in SNF cask monitoring

IV. MOMENTUM INTEGRATED MUON TOMOGRAPHY

2. Results



IV. MOMENTUM INTEGRATED MUON TOMOGRAPHY

2. Results

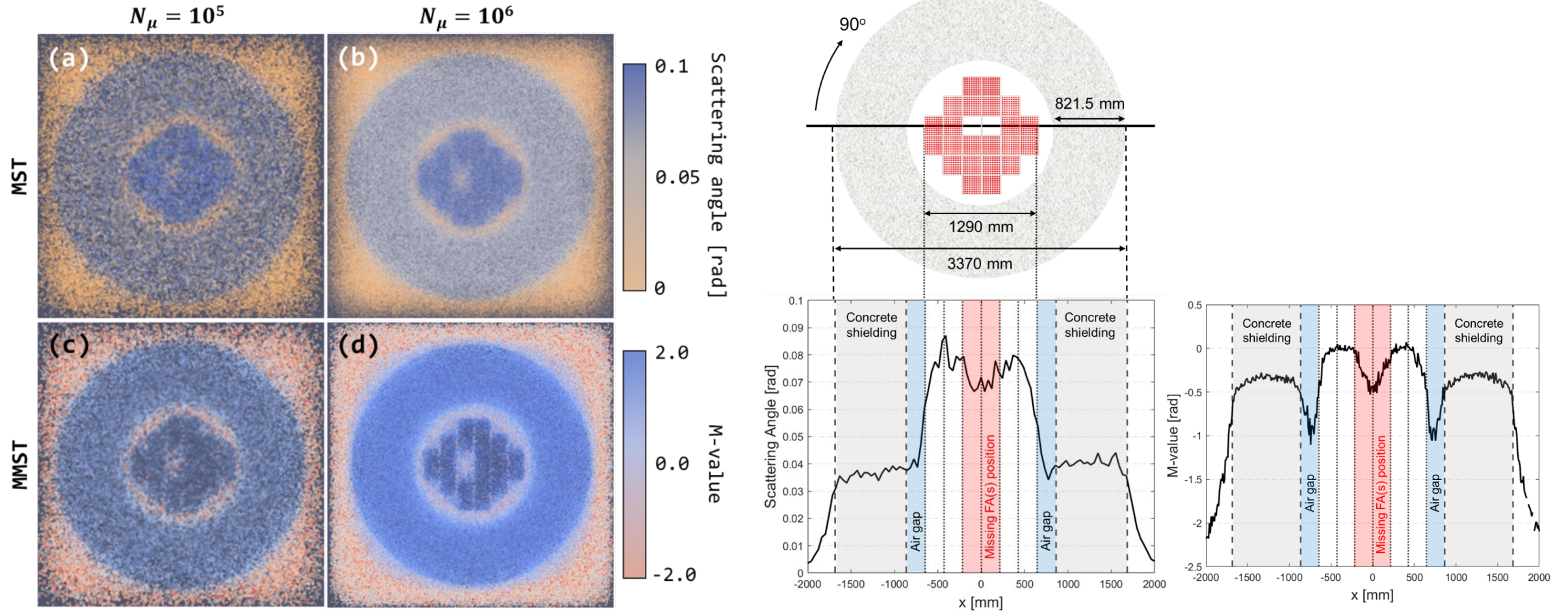


Fig. 4.4 Reconstructed images (left) and systematical analysis of SNF cask using PoCA and mPoCA (right) when two middle FAs are missing

IV. MOMENTUM INTEGRATED MUON TOMOGRAPHY

2. Results

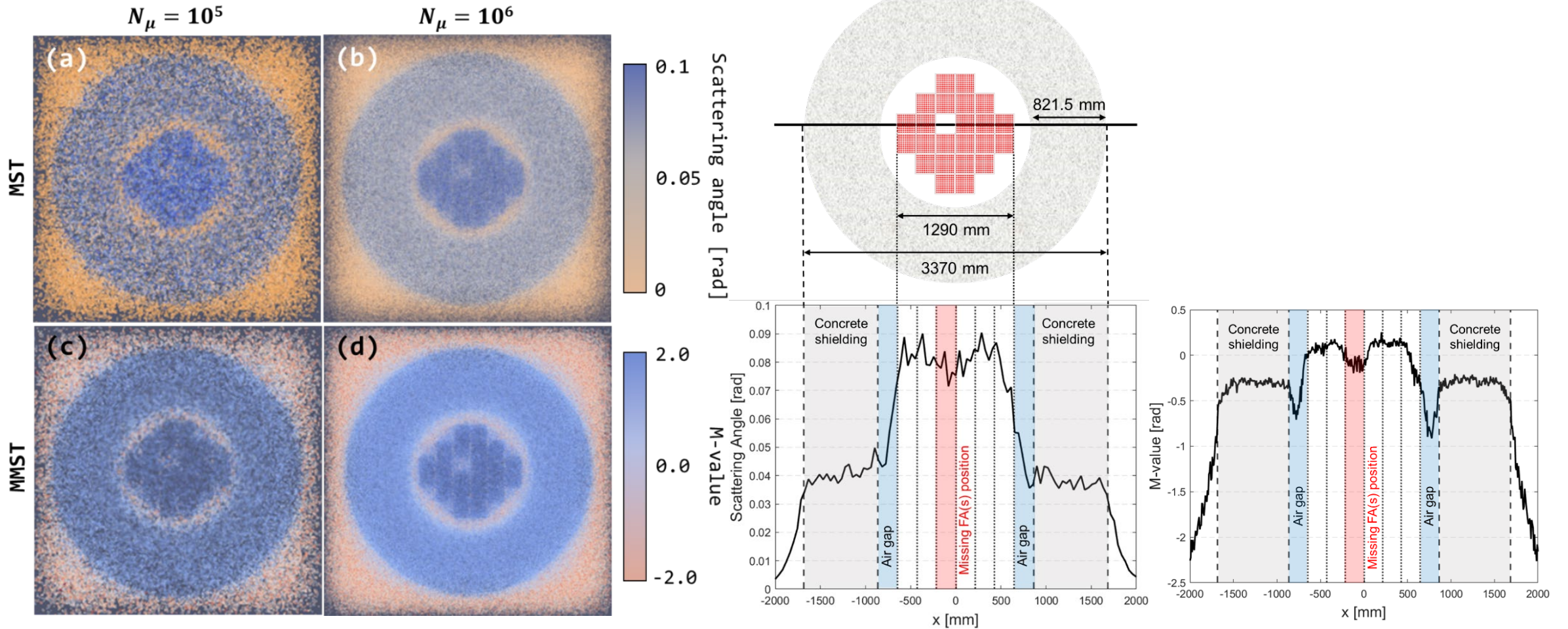


Fig. 4.5 Reconstructed images (left) and systematical analysis of SNF cask using PoCA and mPoCA (right) when one middle FA is missing 40

IV. MOMENTUM INTEGRATED MUON TOMOGRAPHY

2. Results

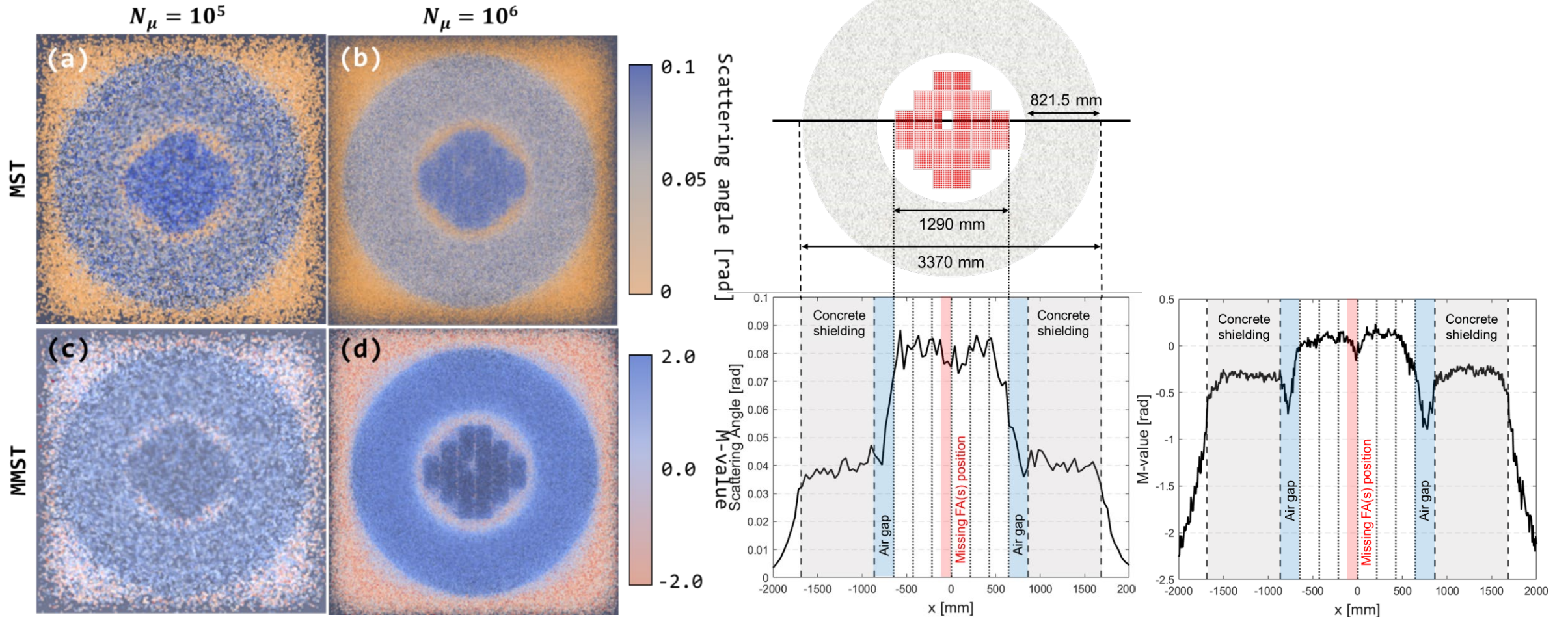


Fig. 4.6 Reconstructed images (left) and systematical analysis of SNF cask using PoCA and mPoCA (right) when a half of middle FA is missing 41

IV. MOMENTUM INTEGRATED MUON TOMOGRAPHY

2. Results

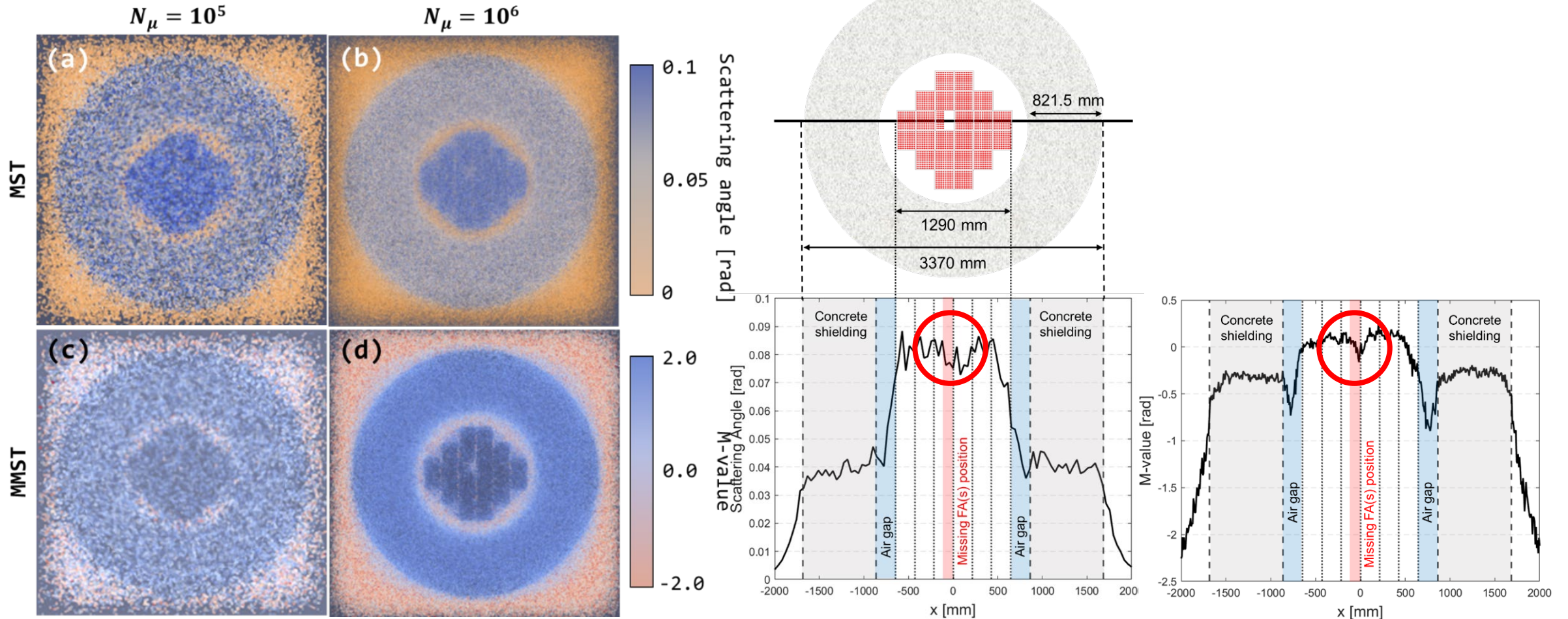


Fig. 4.6 Reconstructed images (left) and systematical analysis of SNF cask using PoCA and mPoCA (right) when a half of middle FA is missing 42

IV. MOMENTUM INTEGRATED MUON TOMOGRAPHY

2. Results

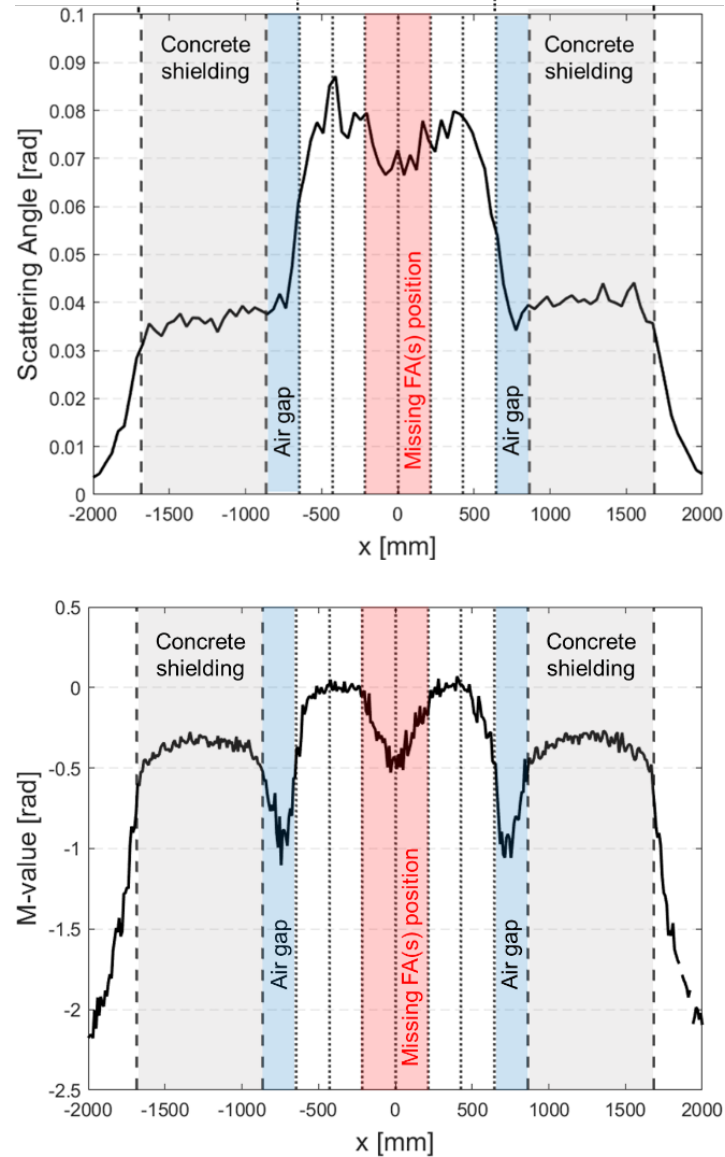
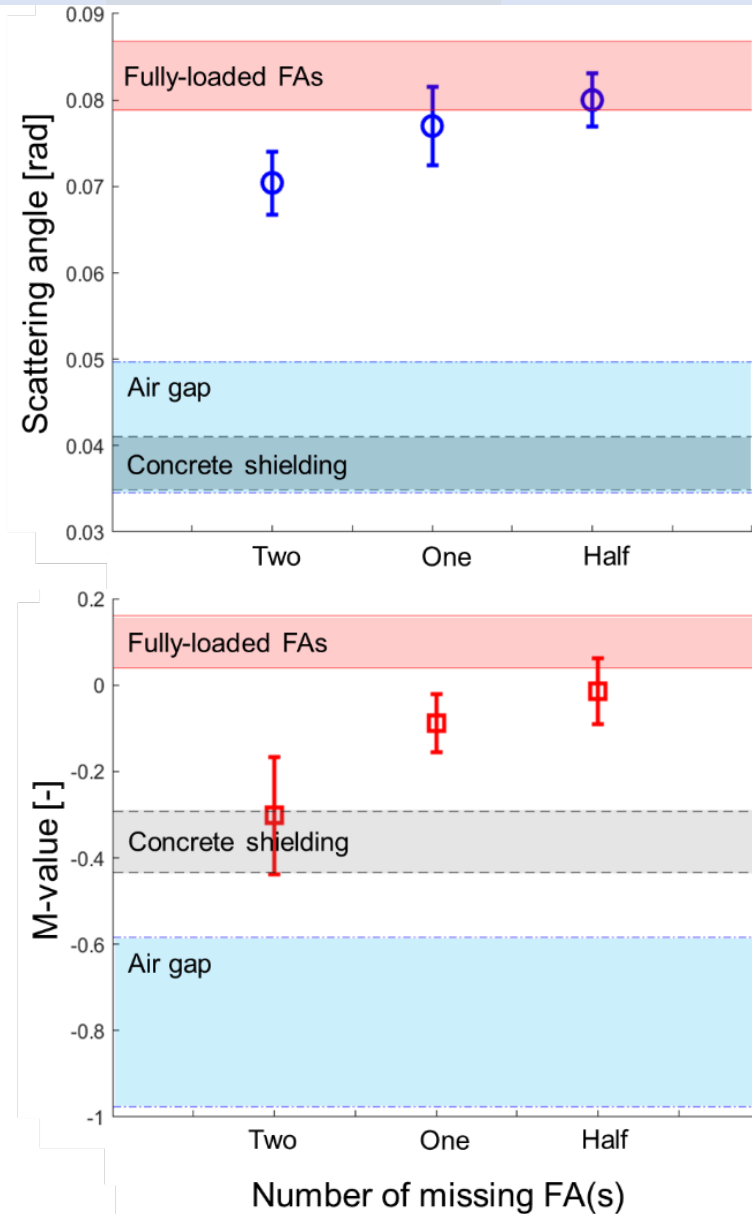


Fig. 4.7 Analysis of missing FA separation capability using PoCA (top) and mPoCA (bottom) algorithms.

IV. MOMENTUM INTEGRATED MUON TOMOGRAPHY

2. Results

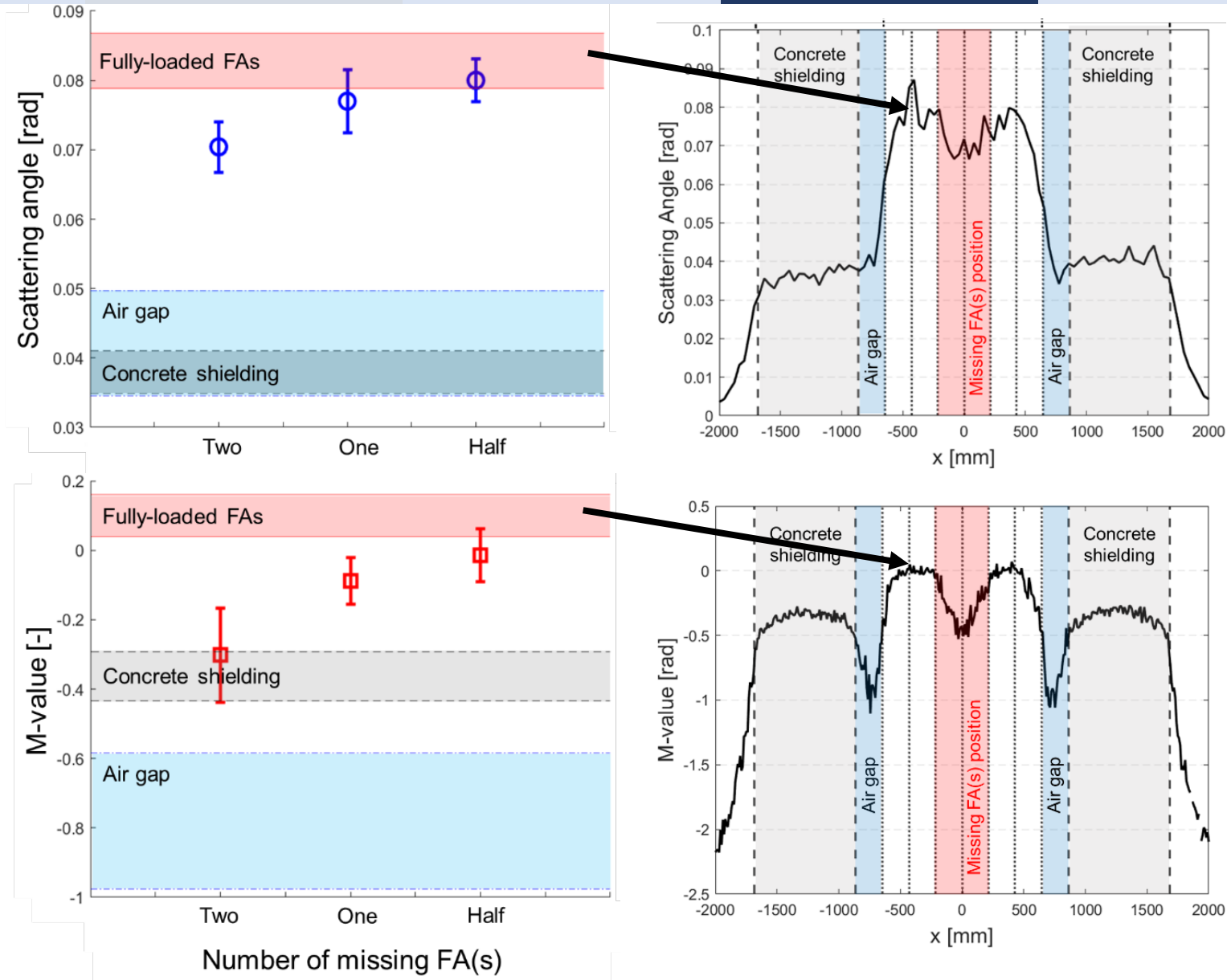


Fig. 4.7 Analysis of missing FA separation capability using PoCA (top) and mPoCA (bottom) algorithms.

IV. MOMENTUM INTEGRATED MUON TOMOGRAPHY

2. Results

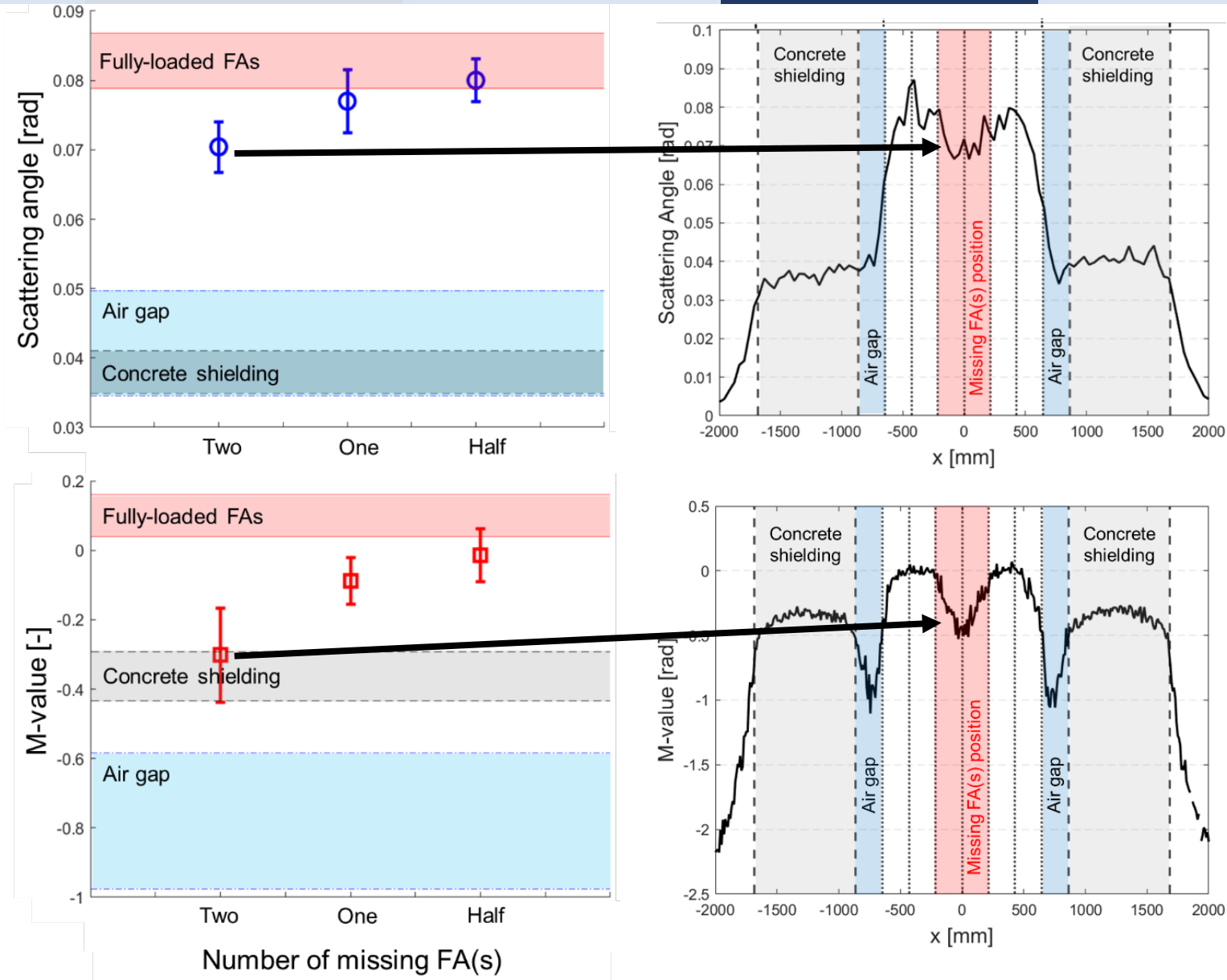


Fig. 4.7 Analysis of missing FA separation capability using PoCA (top) and mPoCA (bottom) algorithms.

IV. MOMENTUM INTEGRATED MUON TOMOGRAPHY

2. Results

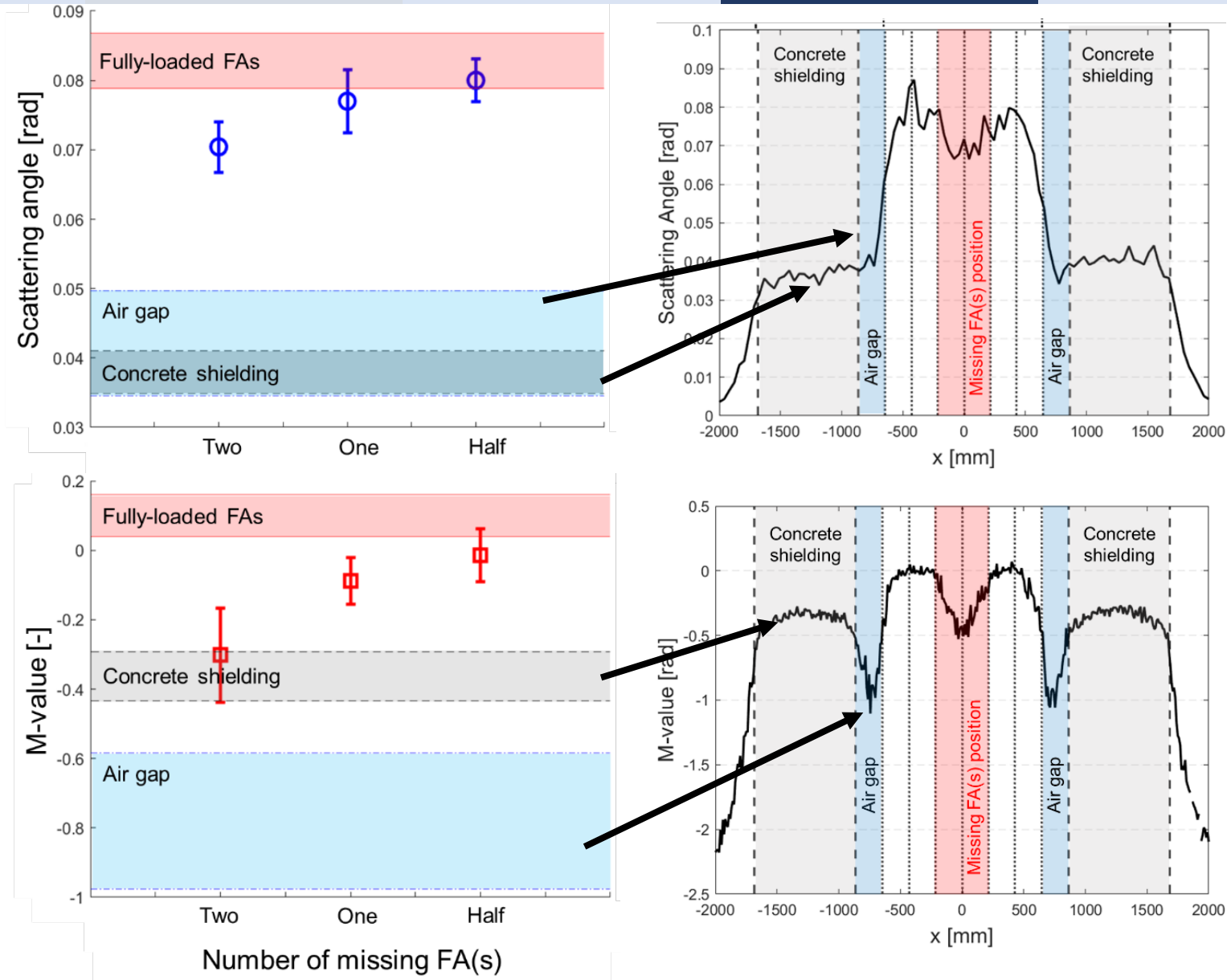


Fig. 4.7 Analysis of missing FA separation capability using PoCA (top) and mPoCA (bottom) algorithms.

A Gas Cherenkov Muon Spectrometer for Nuclear Security Applications

TABLE OF CONTENTS

- I. INTRODUCTION
 - 1. Motivation
 - 2. Problem Statement
 - 3. Research Objective
- II. MUON SPECTROMETER USING GAS CHERENKOV RADIATORS
 - 1. Operational Principle
 - 2. Optical Photon Emission
 - 3. Results
- III. MOMENTUM INTEGRATED IMAGING ALGORITHM
- IV. MOMENTUM INTEGRATED MUON TOMOGRAPHY
 - 1. Implementation of Cherenkov muon spectrometer in SNF monitoring
 - 2. Results
- V. SUMMARY AND CONCLUSION

V. SUMMARY AND CONCLUSION

Muon Spectrometer Using Gas Cherenkov Radiators

1. A glass (SiO_2) and five pressurized gas (CO_2) radiators are used in the prototype.

* Requirements in design

- Easily coupled with existing muon tomography → Simply placed between target object and trackers
- Compact and portable → $\sim 1 \text{ m}^3$
- Light-weight → $< 10\text{kg}$
- Compatible momentum measurement resolution → $\sigma_p/p = 3.35\%$, 21.33% for $N_{\text{rad}} = 100$ and 10 .
- High accuracy → Mean CR $\sim 87\%$
- Preserve incoming and outgoing muon trajectories → Barely interferes initial muon trajectories

2. Although increased N_{rad} improves $\sigma_p/p|_{\text{mean}}$, it will negatively impact the SNR due to the decreased expected Cherenkov signals.

3. To measure energetic muon momentum ($>100 \text{ GeV}/c$), very low gas pressure is **required**.

V. SUMMARY AND CONCLUSION

Momentum Integrated PoCA Algorithm

1. Momentum integrated PoCA imaging algorithm and M-values.
 - A new algorithm does not increase the computational cost.
 - Materials can be classified using M-values which was challenging using muon scattering angles.
 - Imaging resolution is significantly improved.

Momentum Integrated Muon Tomography

1. It enables us to locate two, one, and a half missing FA(s) in a SNF dry cask.
 - Significantly improves the imaging resolution and reduced the required scanning time to find the missing FA by a factor of 10 or more.

List of Publications -- Peer-reviewed Journal Articles

1. J. Bae, S. Chatzidakis, “Momentum Integrated PoCA Algorithm for Muon Scattering Tomography”, *Journal of Imaging* (under review) ← **mPoCA**
2. J. Bae, S. Chatzidakis, “Momentum Integrated Muon Tomography for Spent Nuclear Fuel Monitoring”, *Nuclear Instruments and Methods in Physics Research A* ← **Applications of mPoCA in nuclear material management**
3. J. Bae, S. Chatzidakis, “Generalized mPoCA imaging algorithm for Muon Radiography” (in preparation) ← **Generalized mPoCA**
4. J. Bae, S. Chatzidakis, “Development of compact muon spectrometer using multiple pressurized gas Cherenkov radiators”, *Results in Physics*, **39** (2022)
5. J. Bae and S. Chatzidakis, “Momentum-Dependent Cosmic Ray Muon Computed Tomography using a Fieldable Muon Spectrometer”, *Energies*, **15(7)**, 2666 (2022).
6. J. Bae and S. Chatzidakis, “Fieldable Muon Spectrometer Using Multi-Layer Pressurized Gas Cherenkov Radiators and Its Applications”, *Scientific Reports*, **12**, 2559 (2022).
7. J. Bae and S. Chatzidakis, “A New Semi-Empirical Model for Cosmic Ray Muon Flux Estimation”, *Progress of Theoretical and Experimental Physics*, **ptac016** (2022).
8. J. Bae and R. Bean, “Investigation of Thermohydraulic Limits on Maximum Reactor Power in LEU Plate-Fueled, Pool Type Research Reactor”, *Nuclear Science Engineering* (2022).
9. J. Bae, R. Bean, and R. Abboud, “CFD Analysis of Dry Storage Cask with Advanced Spent Nuclear Fuel Cask Additives”, *Annals of Nuclear Energy*, **145** (2020).

List of Publications -- Oral/Poster Presentations and Conference Proceedings

1. J. Bae, S. Chatzidakis, “Spent Nuclear Fuel Dry Cask Monitoring Using Momentum Integrated Muon Tomography”, International High Level Radioactive Waste Management Conference (embedded in ANS Winter Meeting), Nov 13-17, 2022, Phoenix, AZ.
2. J. Bae, S. Chatzidakis, “Development and Evaluation of Momentum Coupled Muon Scattering Tomography”, IEEE NSS MIC RTSD conference, Nov 05-12, Milano, Italy.
3. J. Bae, S. Chatzidakis, “Non-Linear Cherenkov Muon Spectrometer Using Multi-Layer Pressurized C₃F₈ Gas Radiators”, ANS Annual Meeting, June 12-16, 2022, Anaheim, CA.
4. J. Bae and S. Chatzidakis, “A High-Resolution Muon Spectrometer Using Multi-Layer Gas Cherenkov Radiators”, American Physical Society (APS) March Meeting, Mar 14-18, 2022, Chicago, IL.
5. J. Bae, S. Chatzidakis, “Applied Gas Cherenkov Radiators to Measure Cosmic Ray Muon Momentum”, UKC 2021, Dec 12–15, Anaheim, CA.
6. J. Bae and S. Chatzidakis, “Fieldable Muon Momentum Measurement using Coupled Pressurized Gaseous Cherenkov Detectors”, Trans. Am. Nuc. Soc. 125 (1), 400-403 (2021).

Brauslau Travel Grant

Best Presentation Award

Winner of “Pitch your Thesis” competition

List of Publications -- Oral/Poster Presentations and Conference Proceedings

7. J. Bae and S. Chatzidakis, “Cosmic Muon Momentum Measurement Using the Multiple Pressurized Gaseous Cherenkov Detectors”, IEEE NSS-MIC Conf. Records (2021). IEEE Trainee grant (online)
8. J. Bae and S. Chatzidakis, “The Effect of Cosmic Ray Muon Momentum Measurement for Monitoring Shielded Special Nuclear Materials”, INMM proceedings, (2021).
9. J. Bae, S. Chatzidakis, R. Bean, “Effective Solid Angle Model and Monte Carlo Method: Improved Estimations to Measure Cosmic Muon Intensity at Sea Level in All Zenith Angles”, ICON28 proceedings, 4 (2021). Best Paper Award
10. [INVITED] J. Bae, R. Bean, and R. Abboud, “A Critical and CFD Analysis of a Dry Storage Cask with Advanced Spent Nuclear Fuel Cask Additives”, Waste Management Symposium (WMS), March 2020, Phoenix, AZ, USA. Roy G. Post Scholarship
11. J. Bae and R. Bean, “Analytical Methods in Safeguards for Nuclear Nonproliferation and Complete, Verifiable, Irreversible Denuclearization (CVID) of North Korea”, INMM proceedings (2019).
12. J. Bae, R. Bean, and R. Abboud, “A Criticality Analysis of a Dry Storage Cask with Advanced Nuclear Fuel Cask Additive”, Trans. Am. Nuc. Soc. 118, 147-150 (2018).

Discussion

Junghyun Bae, Ph.D.

School of Nuclear Engineering, Purdue University

Eugene P. Wigner Distinguished Staff Fellow, Oak Ridge National Laboratory

USA

27 July 2022



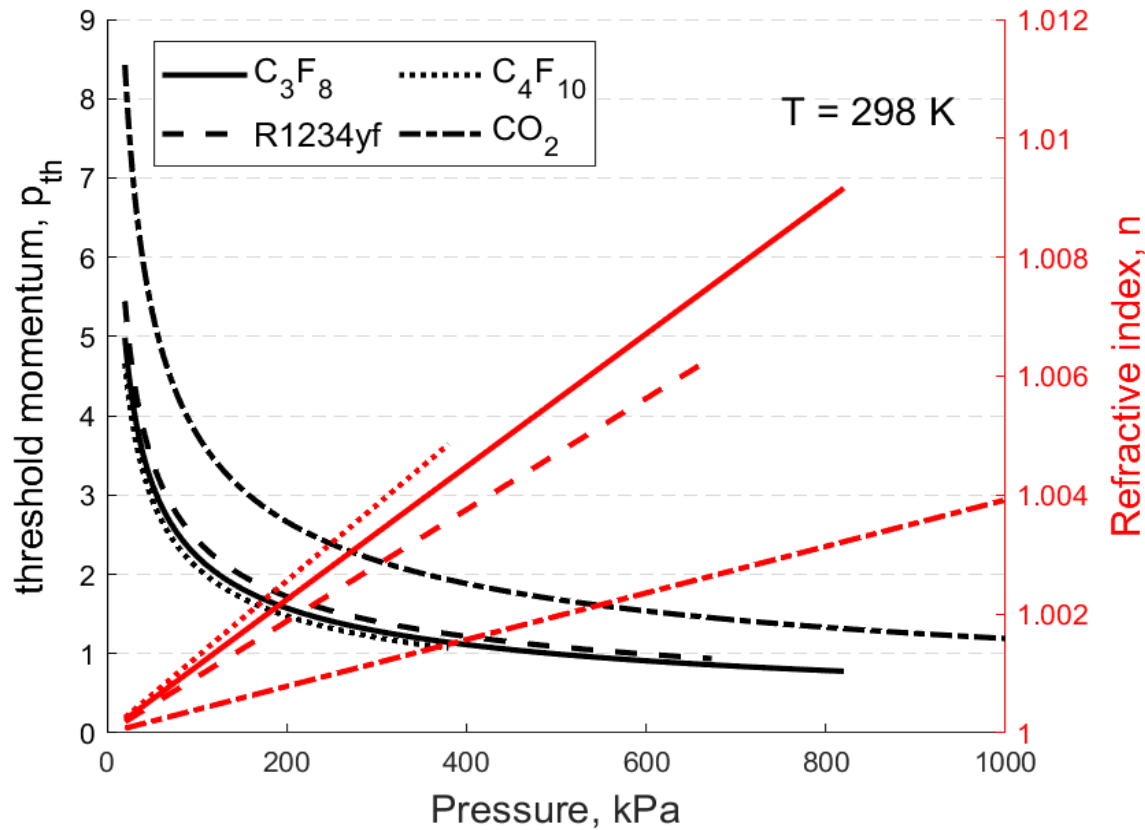
Upcoming Webinars

Date	Title	Presenter
31 August 2022	China's Multi-purpose SMR-ACP100 Design and Project Progress	Dr. Song Danrong, Nuclear Power Institute of China
28 September 2022	Development of In-Service Inspection Rules for Sodium-Cooled Fast Reactors Using the System Based Code Concept	Dr. Shigeru Takaya, JAEA, Japan
26 October 2022	Sodium Integral Effect Test Loop for Safety Simulation and Assessment (STELLA)	Dr. Jewhan LEE , KAERI, Republic of Korea
28 November 2022	Visualization Tool for Comparing Energy Options	Dr. Mark Deinert, Colorado School of Mines, USA

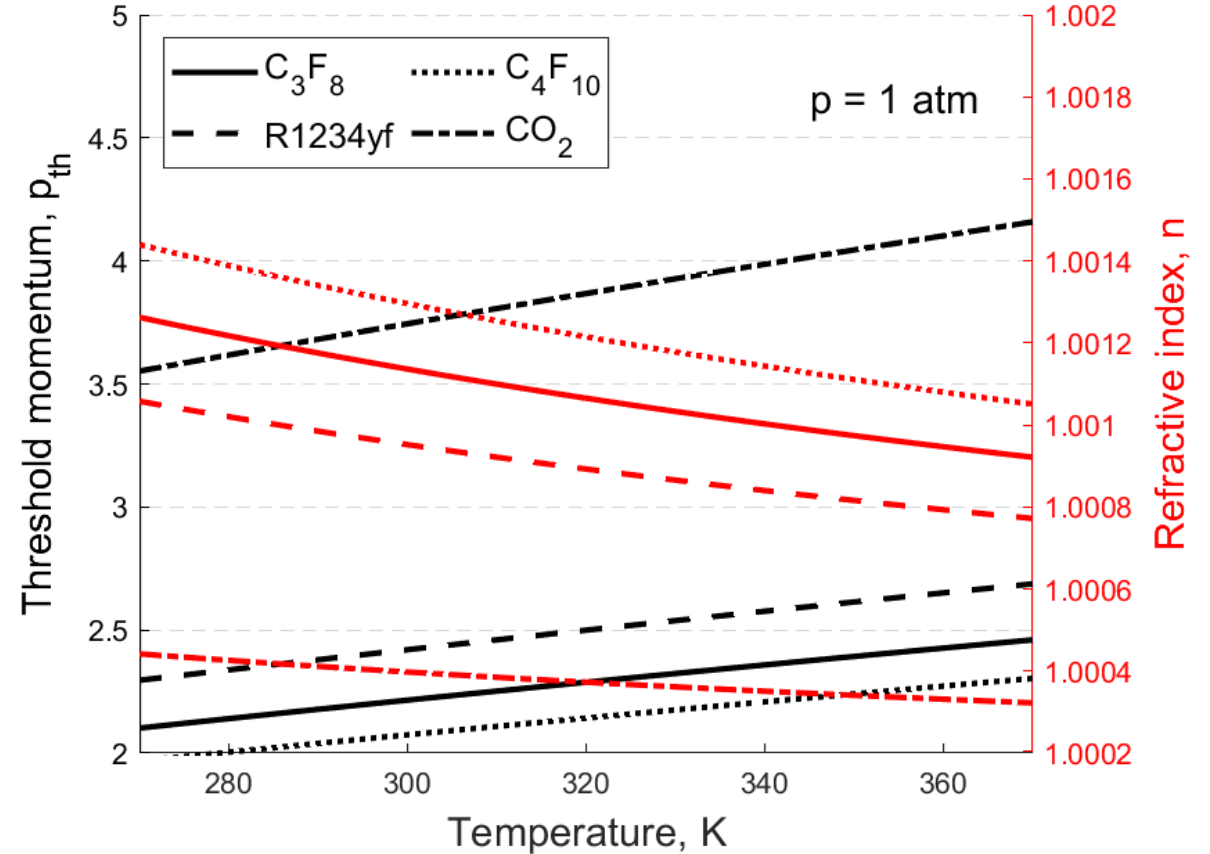
BACKUP SLIDES

II. MUON SPECTROMETER USING GAS CHERENKOV RADIATORS

1) Operational Principle



Pressure vs p_{th} & n



Temperature vs p_{th} & n

Method to differentiate Cherenkov radiation signal from scintillation

